iJRASET
International Journal For Research in
Applied Science and Engineering Technology

INTERNATIONAL JOURNAL FOR RESEARCH

IN APPLIED SCIENCE & ENGINEERING TECHNOLOGY

Volume: 14 **Issue:** VII **Month of publication:** July 2026

DOI: https://doi.org/10.22214/ijraset.2026.84268

www.ijraset.com

Call: 08813907089 | E-mail ID: ijraset@gmail.com

Toward AI-Assisted Conceptual Design of Subsea Inline Structures: Classification and Strain Behaviour of Inline Components during S-Lay Installation

Sreekanth Manakkattil Sivaraman[1], Jagannatha Venkataramana Reddy[2]
Indian Institute of Technology Bombay, Indian Institute of Technology Madras
Subsea Structural Engineer, Subsea Structural Engineer

Abstract: S-lay installation remains the dominant method for offshore pipeline deployment, with inline components — valves, flanges, Inline Tee (ILT) assemblies, and Pipeline End Terminations (PLETs) — increasingly integrated into the continuous pipeline string. As these structures traverse the stinger, the displacement-controlled overbend condition induces strains in the adjacent pipeline that exceed those in plain pipe, a complex and highly localized design condition unique to such subsea assemblies. For a given piping layout, many structural configurations are possible, and identifying the one that minimizes installation strain is a non-trivial search problem that fast-track project schedules rarely allow engineers to conduct systematically; designs are instead adapted from past projects using individual pattern recognition rather than a structured body of design knowledge. This paper is the first in a series developing an AI-assisted conceptual engineering framework for subsea inline structures, using the S-Lay ILT design problem as its case study. It introduces a dual classification system — a physical taxonomy (IW/EA) describing how components connect to the pipeline, and a mechanical taxonomy (Types A, B, C) describing their strain-amplification behaviour — and characterizes each behaviour type through parametric finite element analyses incorporating stinger–pipeline contact modelling. Results identify offset depth and component length as the dominant strain drivers for elevation- and stiffness-type components respectively, quantify the DNV-compliant range for taper transitions, and show that very long components can paradoxically reduce peak strain through dual-roller contact. Together, these findings constitute the design intuition — Steps 1 and 2 of the proposed seven-step framework — needed to support AI-assisted conceptual design of subsea structural assemblies
Keywords: S-lay installation; AI based Subsea ILT design; S-Lay ILT in Overbend; AI in Subsea Engineering, Subsea Structure Design; AI Framework for Structural concept development;

I. INTRODUCTION

A. Complex Structural Assemblies and the Case for AI-Assisted Conceptual Design

Subsea inline structures — ILTs, PLETs, and the piping and structural elements that constitute them — are complex assemblies. Each is built from a distinct combination of components (valves, tees, bulkheads, base structures, top structures, shrouds), and each component carries its own design, fabrication, and procurement considerations. When assembled, these components interact: the mechanical behaviour of the whole is not a simple sum of its parts, particularly under the displacement-controlled overbend condition addressed in this paper. For a given piping and process layout, many structural configurations are possible, and identifying the one that minimizes installation strain is inherently a search problem across a large design space.

Under current fast-track project delivery models, this search is rarely conducted systematically. Engineering teams typically adapt configurations that succeeded on prior projects, applying pattern recognition built from personal experience rather than from a structured body of design knowledge. This is a reasonable response to schedule pressure, but it is also self-limiting: an individual engineer's direct experience covers only a small fraction of the possible component combinations and loading conditions that occur across the industry.

A structured framework — one in which the strain-amplification behaviour of each fundamental component type has been characterized in isolation, and in which these characterizations can be composed to reason about full assemblies — would allow this pattern recognition to be captured, extended, and applied consistently. This is precisely the kind of task suited to AI assistance: an

©IJRASET: All Rights are Reserved

International Journal for Research in Applied Science & Engineering Technology (IJRASET)
ISSN: 2321-9653; IC Value: 45.98; SJ Impact Factor: 7.538
Volume 14 Issue VII July 2026- Available at www.ijraset.com

AI system equipped with a validated, quantitative understanding of component-level behaviour can act as a first-pass concept generator, proposing candidate configurations and flagging likely governing mechanisms before any finite element analysis is performed, leaving the engineer to review, refine, and validate rather than search from a blank page.

Realizing this capability requires that the underlying engineering knowledge exist first, in a form that is both rigorous enough to be trustworthy and structured enough to be machine-usable. This paper covers the initial steps in that programme, using the S-Lay ILT design problem as the practical case study through which the framework is developed. Fig. 1 presents the complete seven-step AI-assisted conceptual engineering development programme; the two steps addressed in this present paper — Component Classification and Design Intuition — are highlighted, with Steps 3 through 7 defining the roadmap for the papers that follow in this series.

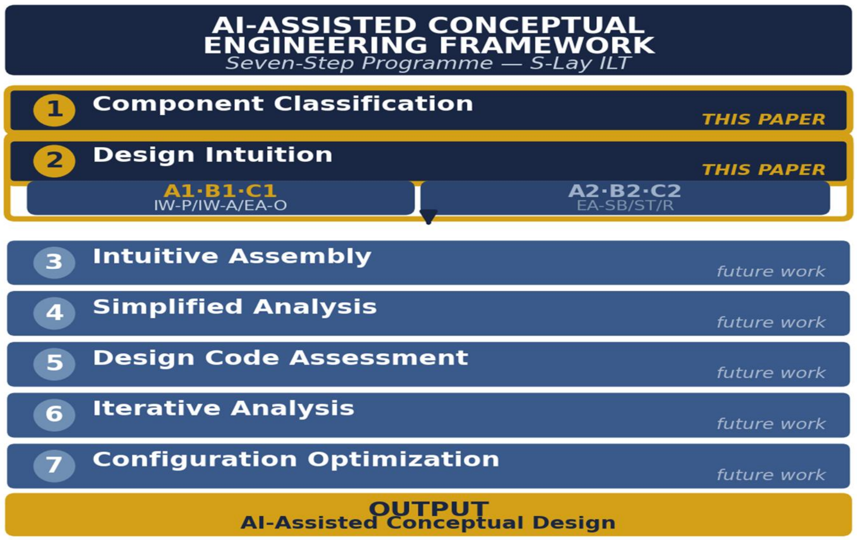

Fig. 1. Engineering Framework : AI Assisted Conceptual Design

B. Installation Methods and the S-Lay Overbend

Offshore oil and gas fields rely on subsea pipelines to transport production fluids from wellheads to processing facilities. Three principal pipelay installation methods are used in practice: S-lay, J-lay and reel-lay. In S-lay, the pipe is assembled on the vessel deck and fed over a curved stinger at the stern, forming an overbend above the stinger and a sagbend catenary below. J-lay uses near-vertical departure with a single sagbend and no overbend. Reel-lay pre-fabricates pipe onshore and pays it out through a straightener at sea.

S-lay is the dominant method for medium to large diameter pipelines across a broad depth range. Multiple weld stations operate simultaneously on the stable vessel deck, enabling continuous pipeline assembly at high throughput. The adjustable stinger radius allows operation from shallow coastal water to beyond 2,000 m on semi-submersible vessels [1], [2]. Refer Fig. 2 for illustrative overview of the 3 methods.

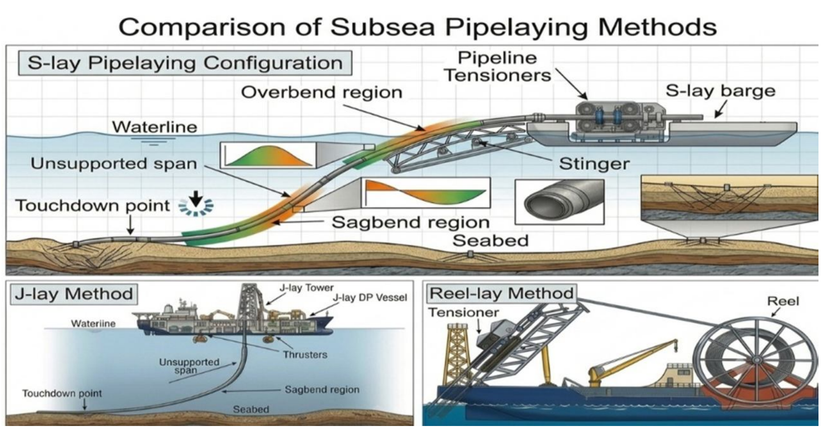

Fig. 2. The three principal installation methods. Only S-lay produces a discrete-roller overbend — the loading condition studied here.

International Journal for Research in Applied Science & Engineering Technology (IJRASET)
ISSN: 2321-9653; IC Value: 45.98; SJ Impact Factor: 7.538
Volume 14 Issue VII July 2026- Available at www.ijraset.com

In the S-Lay installation method, the overbend region is the section of pipeline between the vessel and the point where the pipe leaves the stinger and enters the water. In this region, the pipeline experiences positive curvature (concave upward) as it transitions from a near-horizontal position on the vessel to a downward slope toward the seabed. The stinger supports the pipeline in the overbend, ensuring that the curvature remains smooth and that bending stresses and strains stay within allowable limits. This region is critical because excessive curvature can lead to local yielding, buckling, or coating damage.

C. S-Lay Vessel and Stinger

An S-Lay vessel is a specialized offshore installation ship used to lay pipelines on the seabed in shallow to deep waters. Onboard, the pipeline is assembled horizontally along the deck through welding stations and then gradually lowered into the sea in an "S-shaped" profile. A critical component of this system is the stinger, which is a long, curved or trussed structure extending from the stern of the vessel. The stinger supports the pipeline as it leaves the vessel and carefully controls its curvature in the overbend region, ensuring that bending stresses remain within allowable limits. By providing a smooth transition from the vessel to the water, the stinger prevents excessive deformation or damage to the pipe during installation and allows safe and efficient lay operations across varying water depths. Framed assembly of rotating rollers are installed at regular intervals on a stinger to support, guide, and control the curvature of a pipeline while minimizing friction and damage during installation.

The curvature of a stinger in an S-Lay vessel is carefully controlled through a combination of structural geometry and adjustable mechanical systems to maintain safe pipe bending stresses. Refer Fig. 3 for representative images of Stinger, Roller box and their overall arrangement.

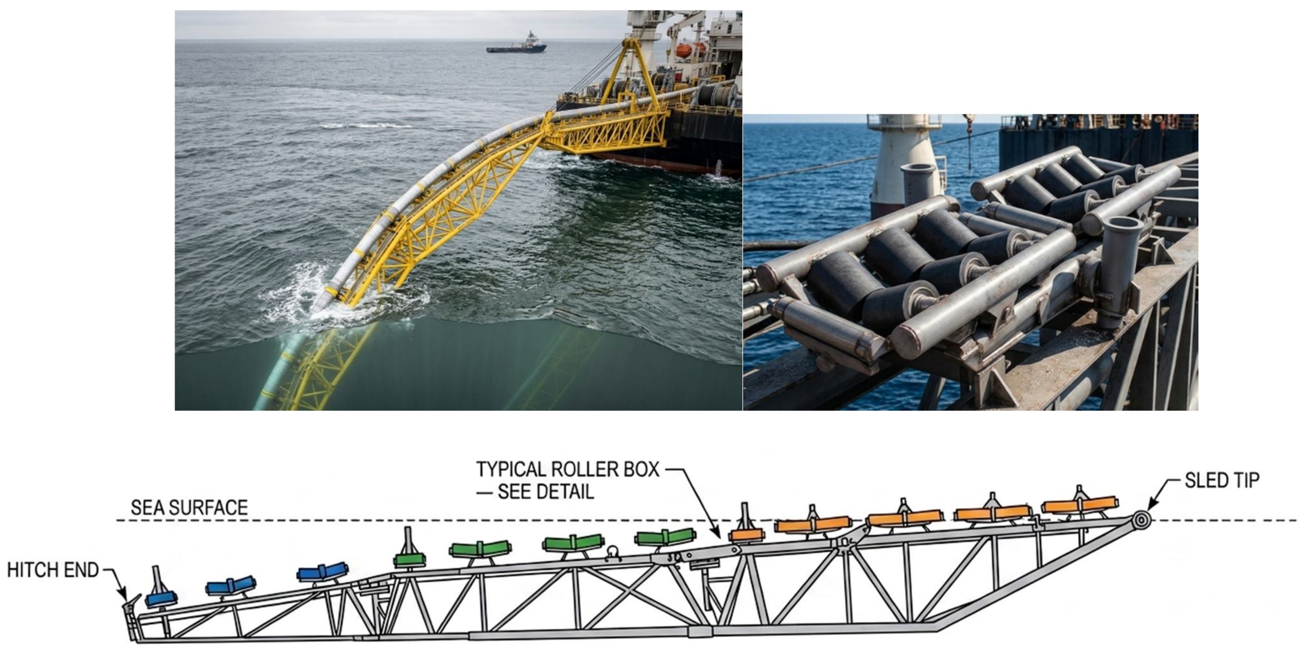

Fig. 3. Typical S-Lay Vessel Stinger , Roller Box and Roller Arrangement Illustration (Representative Images)

Roller boxes on a stinger are typically connected using hinged (articulated) connections to allow controlled movement and alignment with the stinger curvature. These hinges enable each roller box to rotate slightly relative to the stinger structure, ensuring that the rollers remain properly aligned with the pipeline as it follows the curved profile. This flexibility helps to maintain continuous contact between the pipe and rollers, reducing localized stresses and preventing uneven loading. Additionally, hinged connections accommodate small geometric variations and dynamic movements during installation, improving load distribution and protecting the pipeline coating. Typically roller boxes are spaced at 5 to 9m intervals.

The S-Lay overbend region has been extensively studied due to its critical role in controlling pipeline stresses during installation. Early works such as Palmer and King [2][1] established the fundamental understanding of pipeline catenary behaviour and the interaction between tension, bending, and stinger geometry. Subsequent research has focused on improving analytical and numerical models to capture the complex combined loading conditions in the overbend, including axial tension, bending moment, roller

ISSN: 2321-9653; IC Value: 45.98; SJ Impact Factor: 7.538
Volume 14 Issue VII July 2026- Available at www.ijraset.com

reactions, and vessel motions. Studies by Xie et al. [9],[10], highlighted the importance of real-time monitoring of overbend strain, noting that this region is often subject to significant uncertainty due to dynamic effects. Numerical and finite element investigations, such as those by Ivić [11] and Xu [12] demonstrated that pipeline response is highly sensitive to parameters like stinger angle, roller spacing, and applied tension, and that environmental loading (e.g., waves) can significantly influence stress levels. More recent work by Jansen [17] emphasizes the partially displacement-controlled nature of the overbend, challenging simplified design assumptions and improving buckling assessment accuracy. Optimization-based studies further show that installation configuration plays a dominant role in minimizing stresses and ensuring safe operations. Overall, the literature converges on the need for integrated design approaches combining analytical models, numerical simulation, and real-time monitoring to accurately predict and control overbend behaviour in modern deepwater S-Lay installations

D. Inline Structures and the Stinger Passage Event

Subsea field architecture requires reliable connection points along pipelines to enable flow distribution, tie-ins, and integration of subsea production systems. At intermediate locations, Inline Tee (ILT) assemblies are used to provide branch connections for additional flowlines, well tie-ins, or future expansion, while at the ends of pipelines, Pipeline End Terminations (PLETs) serve as interface structures for connection to subsea manifolds, risers, or jumpers. These inline components are essential because modern subsea developments rarely consist of single, continuous pipelines; instead, they involve complex networks of wells, manifolds, and processing units, all requiring controlled flow routing and isolation capability. The scale of such deployments is significant: a single deepwater field installation may involve more than 20 inline structures connected along multiple flowline loops, with individual structure weights reaching 20 metric tons or more [6].

During S-Lay installation, ILTs and PLETs are fabricated, welded, and integrated into the pipeline string on the firing line, similar to standard pipe joints. Once incorporated, they pass through the tensioner and stinger system, which must be capable of handling their increased weight, stiffness, and geometric irregularities compared to plain pipe. As the pipeline is deployed, these structures also traverse the stinger and overbend region, where they are subjected to combined loading conditions including axial tension, bending, and localized roller contact forces. This makes their installation more critical than that of uniform pipe sections, as the stiffness discontinuity and mass concentration can lead to stress concentrations, higher bending strains, and potential misalignment.

A typical and simplistic representative model of an Inline TEE structure along with an illustrative representation of its overbend passage is shown in Fig. 4. This is one of the several possible situations discussed later in this paper. In this type of structural arrangement, if the structure is rigidly attached to the pipeline, there can be strain increment on the pipeline outside the structural connections.

Other than TEEs, there are other possible inline components like Valves, Flanges etc. When such components are present in the header pipeline, a shell type structure is required at their base (Base Structure) to protect the component during passage over the Stinger and later while installed on the seabed. Refer Fig. 5 for examples of such assemblies. As they pass over the Stinger, the Pipeline will be elevated which causes local increase in curvature of pipeline. Some ILT structures also need such a Base structure, usually when they have a large OD component on the header line. Refer Fig. 6 for example.

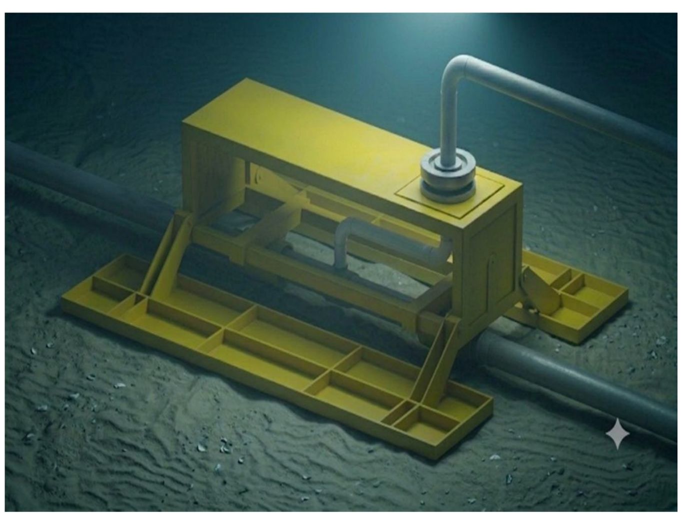

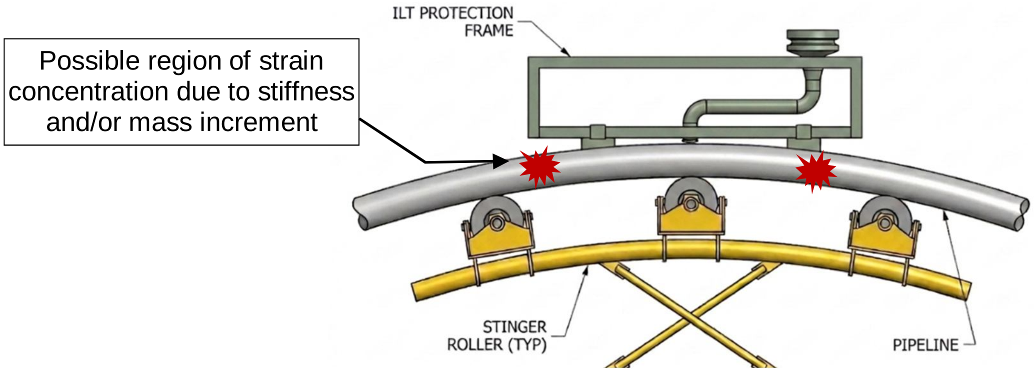

Fig. 4. A Typical Inline Tee Structure and its overbend passage (Representative Images)

Other than TEEs where an external pipe connects to the main pipeline, there are also other possible components like Valves and Flanges. Typically a Base structure is used to form a protective shell surface below the component, and this Base structure is attached to the pipeline. This can cause the Pipeline to locally elevate at a roller, causing higher strains at some regions. Base Structure is also required in ILT structures with Valves on header lines. Refer Fig. 5 and Fig. 6 for schematic overviews.

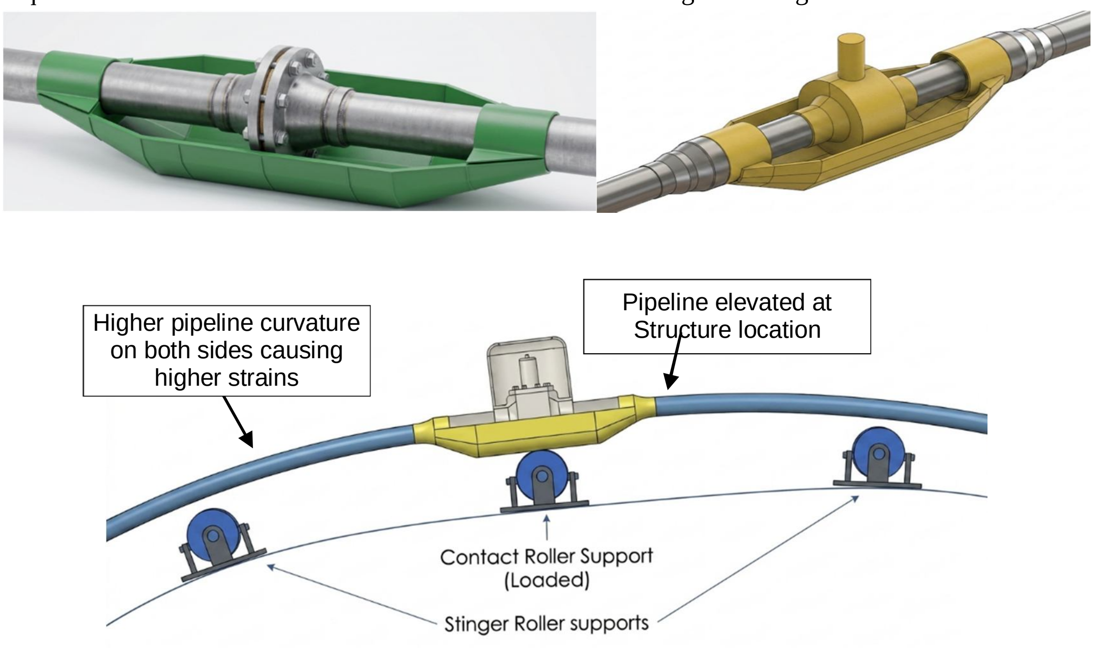

Fig. 5. Other Types of Inline Structures with elevated Bases and their overbend passage (Representative Images)

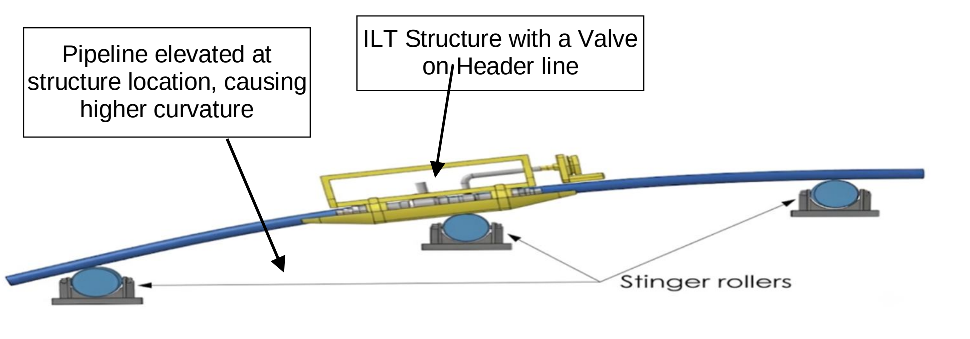

Fig. 6. ILT Structure with a Large OD component on Header line

International Journal for Research in Applied Science & Engineering Technology (IJRASET)
ISSN: 2321-9653; IC Value: 45.98; SJ Impact Factor: 7.538
Volume 14 Issue VII July 2026- Available at www.ijraset.com

The need for inline components arises from several operational and design requirements. They enable flexible field layout, allowing pipelines to connect multiple wells and facilities without requiring separate lines for each connection. They also provide future tie-in capability, which is particularly important for phased field development. Additionally, ILTs and PLETs facilitate installation and commissioning operations, including pressure testing, pigging, and connection to subsea infrastructure. However, their presence introduces significant challenges during installation, requiring detailed pipelay analysis, careful positioning along the firing line, and sometimes additional installation aids such as buoyancy modules or support frames to ensure safe passage over the stinger.

In summary, inline pipeline components such as ILTs and PLETs are indispensable elements of subsea systems, enabling connectivity and operational flexibility, but they also represent critical design and installation challenges, particularly in the S-Lay overbend region where structural demands are highest.

E. Inline Components and Structural Assemblies — A Physical Taxonomy

No unified classification exists in the subsea installation literature for inline pipeline hardware from a mechanical-behaviour perspective. Component descriptions in the industry follow process function — valve, Tee, flange, bulkhead — rather than the properties that govern overbend strain during installation: connection method to the pipeline string, contact elevation at stinger rollers, and local bending stiffness. The dual-classification system introduced here is purpose-built to bridge the hardware design domain (DNV-ST-F101, ASME VIII) and the S-lay installation analysis domain.

Its two layers are:

- Physical IW/EA classification (See TABLE I), which captures how each component connects to or attaches to the pipeline string; and the
- Mechanical Types A–C (See TABLE II), which capture the independent strain-amplification mechanisms active during stinger passage.
- The mapping between the two — given in TABLE III — enables a practitioner to identify the governing mechanical type for any hardware configuration before detailed finite-element analysis is required

This type of a classification of components with **Item Coding** also helps to modularize the design and use AI assisted conceptual and optimization design methods.

The hardware installed inline in a subsea pipeline falls into two fundamentally different categories.

- Inline Welded (IW) components interrupt the pipeline string and are joined by full-penetration girth butt welds at each end.
- Externally Attached (EA) components connect to the pipeline OD or to an IW-A Boss without cutting the string.

Within each group, sub-types are identified by a two-letter code. Most ILT and PLET installations combine components from both groups acting together.

TABLE I. PHYSICAL CLASSIFICATION OF INLINE HARDWARE (IW / EA NOMENCLATURE)

Group Code	Connection Method	Description	Item Code	Connection to Pipeline
IW (Inline Welded)	Full-penetration girth butt weld (with tapered NIB) at each end. Pipeline is cut; component becomes part of the string.	Piping Components (Valve, Flange, TEE etc)	IW-P	Full-penetration girth butt weld inline into string. Large OD requires EA-O or EA-SB for roller management.
		Anchoring Components	IW-A	Welded inline. Provides the connection point for EA-SB/ST. Large OD (eg: PIP bulkhead) requires EA-O or EA-SB for roller management.
		Branch Piping	IW-B	Welded inline. Connector at the end of branch need EA-ST
EA (Externally Attached)	Externally attached built up Structure – Frame or Shell (EA-S)	Base Structure	EA-SB	Connected to pipeline at 1 or more locations via IW-A or EA-R. Runs below pipeline and below inline piping components.
		Top Structure	EA-ST	Connected to pipeline at 1 or more locations via IW-A Boss or EA-R. Runs on top of the pipeline, usually cover the piping components
	Other Externally attached component	EA — Ring	EA-R	Sleeve pipe with encircling fillet girth weld to pipeline OD. Provides connection point for EA-S when no IW-A is present.
		EA — Offset Element (Shroud)	EA-O	No structural weld-line connection. Geometric contact only Used to provide a an alternative contact surface with rollers, usually to elevate and control pipeline curvature
		Misc Other		Includes components such as Boss pipes fixed to Bulkheads

International Journal for Research in Applied Science & Engineering Technology (IJRASET)
ISSN: 2321-9653; IC Value: 45.98; SJ Impact Factor: 7.538
Volume 14 Issue VII July 2026- Available at www.ijraset.com

IW-P and IW-A components share the same connection geometry — a full-penetration girth butt weld on the NIB edge,, followed inward by a Tapered Transition to the body thickness, per DNV-ST-F101 §5.6 — but they differ in function. IW-P carries the process fluid; IW-A provides the anchor bulkhead to which EA-SB/ST attaches. EA-R is an alternative to IW-A for attaching EA-S where interrupting the pipeline string is not practical. EA-O components carry no weld-line loads; they redistribute roller contact forces upward through geometric offset only.

- Fig. 7 presents an ILT Structural assembly including most of the components mentioned above.
- Fig. 8 presents ILT variation in the type of connector – Horizontal or Vertical.
- Fig. 9 presents some of the non-ILT Inline structures. Presence of High OD components on the header pipeline requires elevation, as discussed in previous section.

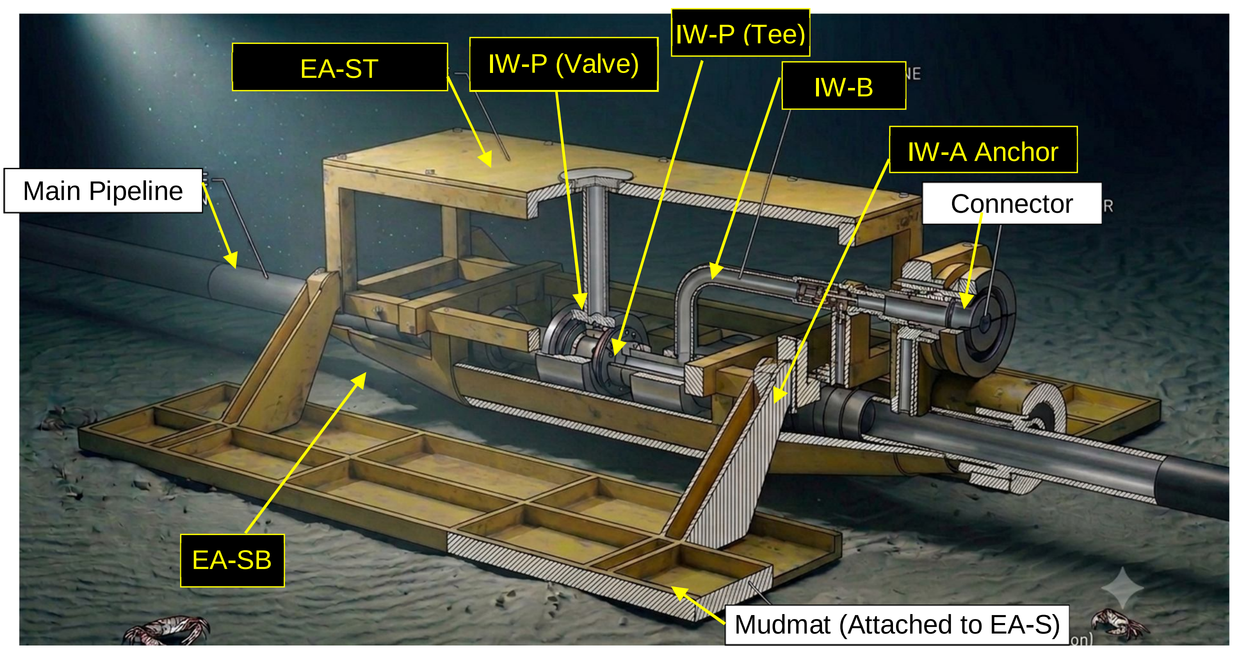

Fig. 7. A Typical ILT Assembly (Representative Image)

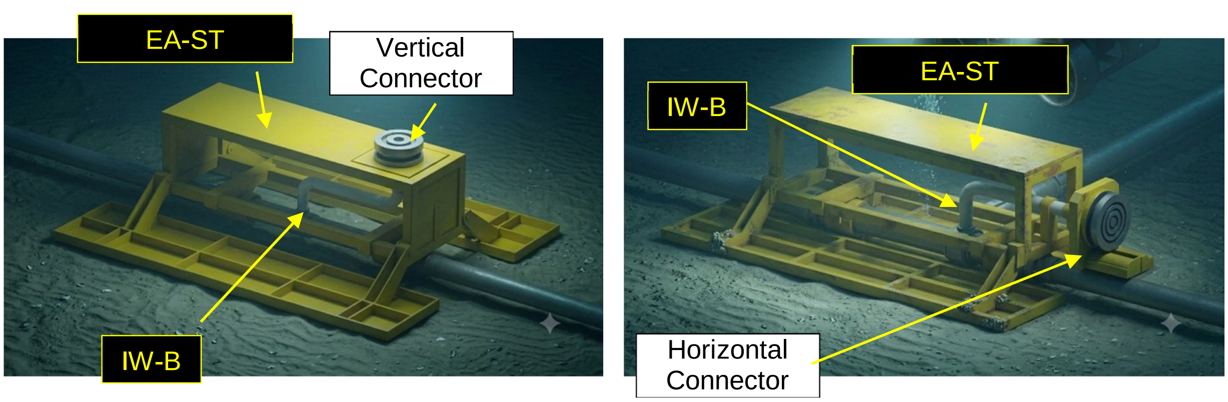

Fig. 8. ILT without Base Structure – Connector Type Variation (Representative Image)

International Journal for Research in Applied Science & Engineering Technology (IJRASET)
ISSN: 2321-9653; IC Value: 45.98; SJ Impact Factor: 7.538
Volume 14 Issue VII July 2026- Available at www.ijraset.com

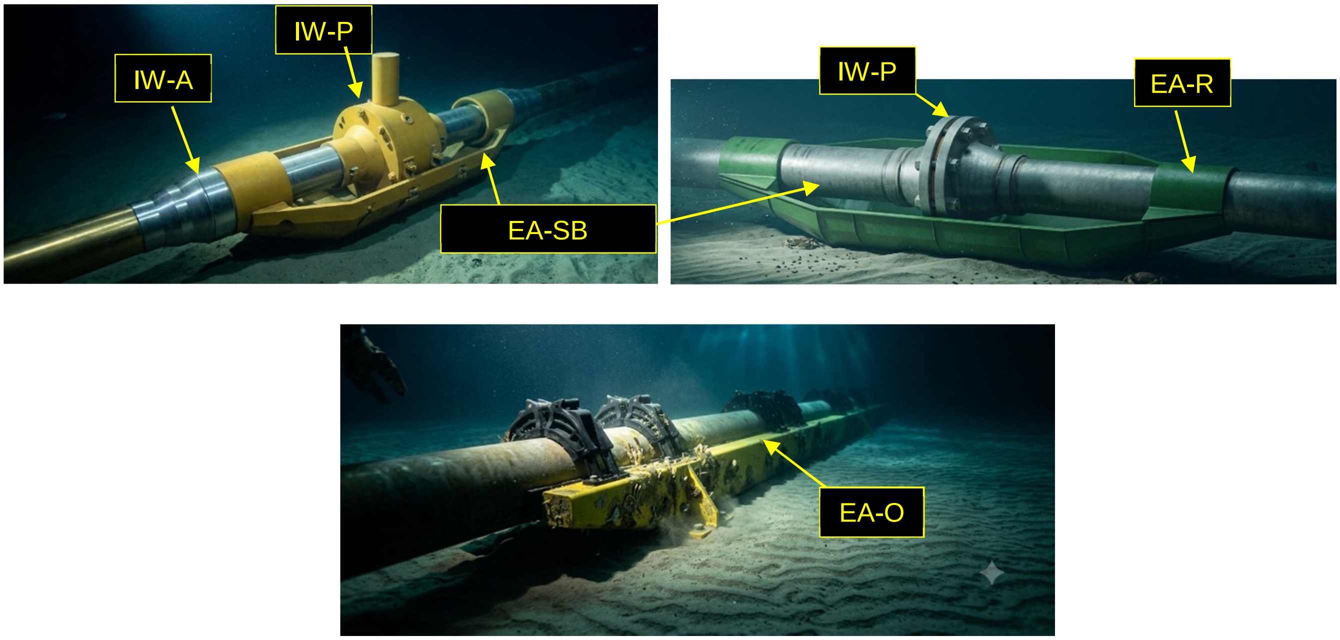

Fig. 9. Misc. Non-ILT Inline Structures (Representative Image)

- Fig. 10 and Fig. 11 presents examples of Anchor bulkhead components. PIP Bulkhead is the most common and robust method of anchoring Structures to pipeline. Such connection has the capability to transfer large loads with minimal secondary stress and fatigue issues.
- Fig. 12 presents example of using Encircling rings to attach structure to pipeline. Such connection is not so common due to some technical issues. Refer discussion later in this document

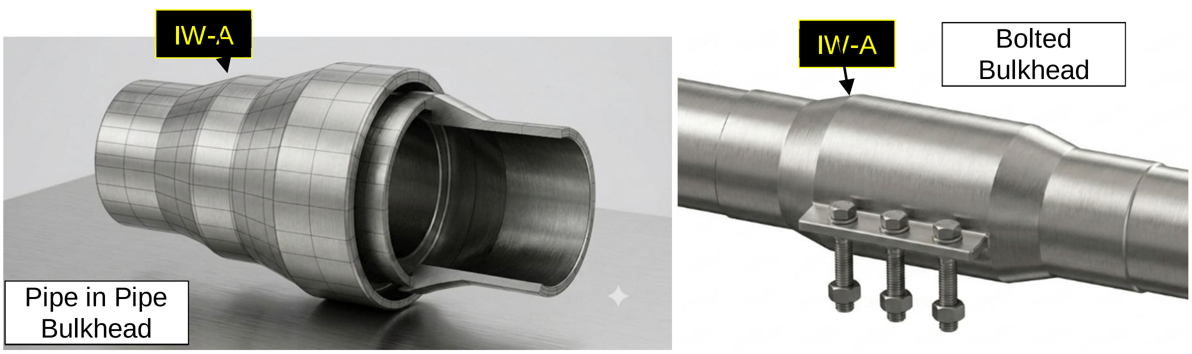

Fig. 10. Example IW Anchoring Components (Representative Image)

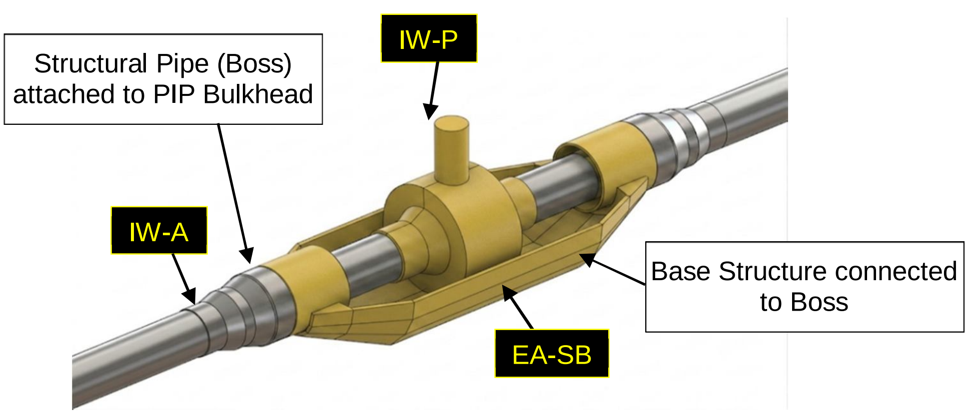

Fig. 11. Example of PIP Bulkhead usage to anchor structure to Pipeline (Representative Image)

International Journal for Research in Applied Science & Engineering Technology (IJRASET)
ISSN: 2321-9653; IC Value: 45.98; SJ Impact Factor: 7.538
Volume 14 Issue VII July 2026- Available at www.ijraset.com

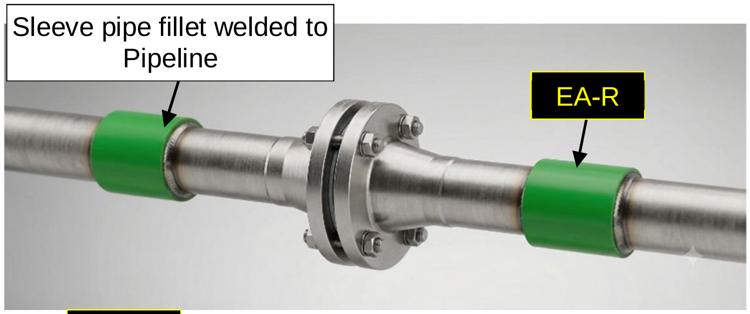

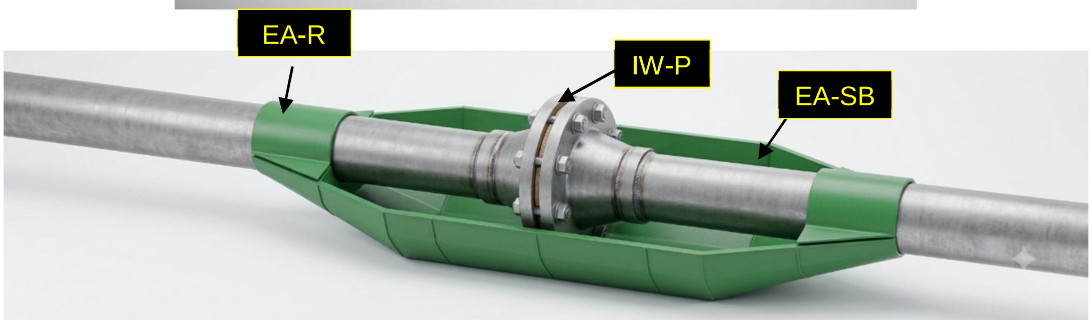

Fig. 12. Example of External sleeve usage to anchor structure to Pipeline (Representative Image)

- Fig. 13 presents examples of attaching Plastic shrouds on the pipeline to create and additional contact surface. This can be used to control curvature of the pipeline and thus control the strains. This can also help pass non-uniform shaped inline components to pass over the roller surfaces by providing smooth contact surfaces cover the non-uniform shapes.

Fig. 13. Examples of Shroud Attachment to Pipeline (Representative Image)

TABLE II. MECHANICAL BEHAVIOUR CLASSIFICATION (TYPES A–C) FOR OVERBEND STRAIN ANALYSIS.

Type	Name	Stiffness Effect	Elevation Effect	Description
A (A1/A2)	Stiffness-dominant	Significant	Minor	• Typically, all IW components have this effect due to them having higher wall thickness than pipeline • EA-S components may or may not show this behaviour, depending on the type of connection to Pipeline (Rigid or Flexible) • A Stiff inline component or a section of pipeline with restricted bending causes strain concentrations in adjoining regions. Component length, stiffness and spacing drives the magnitude of strain increment.

				• There are 2 subtypes o **A1**: Uniformly distributed stiffness (eg: thick component) o **A2**: Stiffness concentrated at connection points (eg: EA-S or IW-B rigidly connected to pipeline at distinct points) • Refer Fig. 14
B (B1/B2)	Elevation-dominant	Negligible	Significant	• This type of behaviour is shown by components that purely elevates the pipeline on stinger, and does not bend with the pipeline or restrict its bending. • The component changes the curvature of pipeline bending across the stinger and therefore it is typically used to avoid sharp changes of curvature
				• There are 2 subtypes o **B1**: Component applies elevation to pipeline directly above it (eg: Shroud) o **B2**: Component applies elevation at distinct points where its attached, without restricting bending (eg: EA-SB) • Refer Fig. 15
C	Combined	Significant	Significant	• This is a combination of behaviours above, and has several possibilities. Typically shown by assembled inline structures
				• Broadly classified into 2 Sub types o **C1**: Combination of A1 and B1 o **C2**: Any other combinations between A and B • Refer Fig. 16 for example of C1. Behaviour type C2 is exhibited by several options and need dedicated work on its own

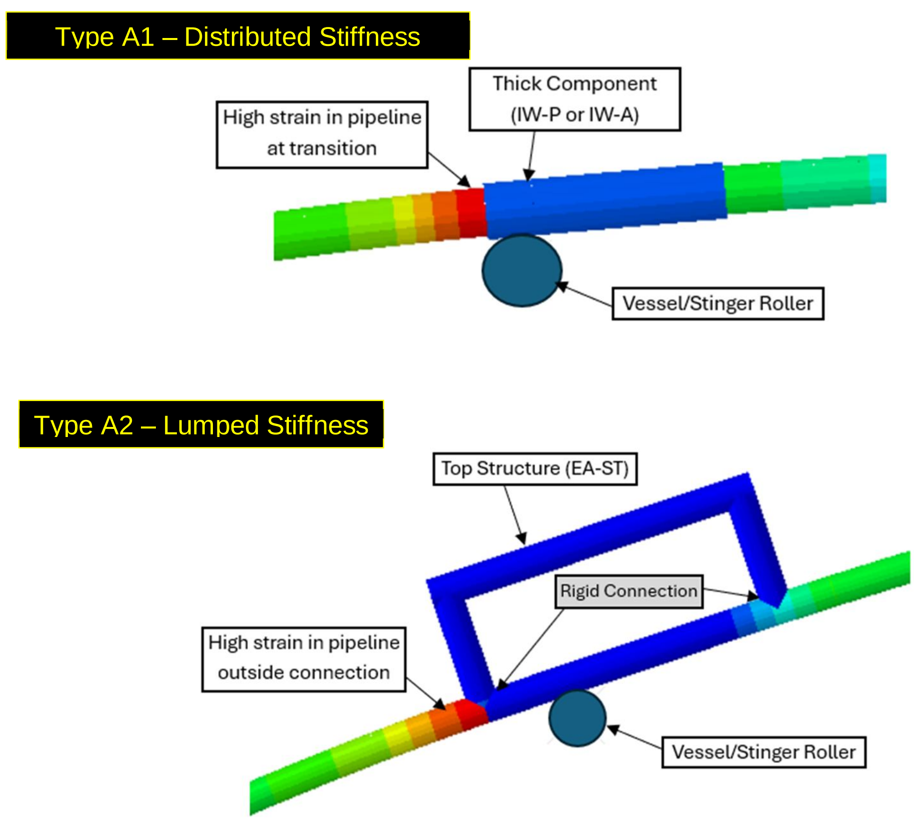

Fig. 14. Example of Type A Mechanical Behaviour

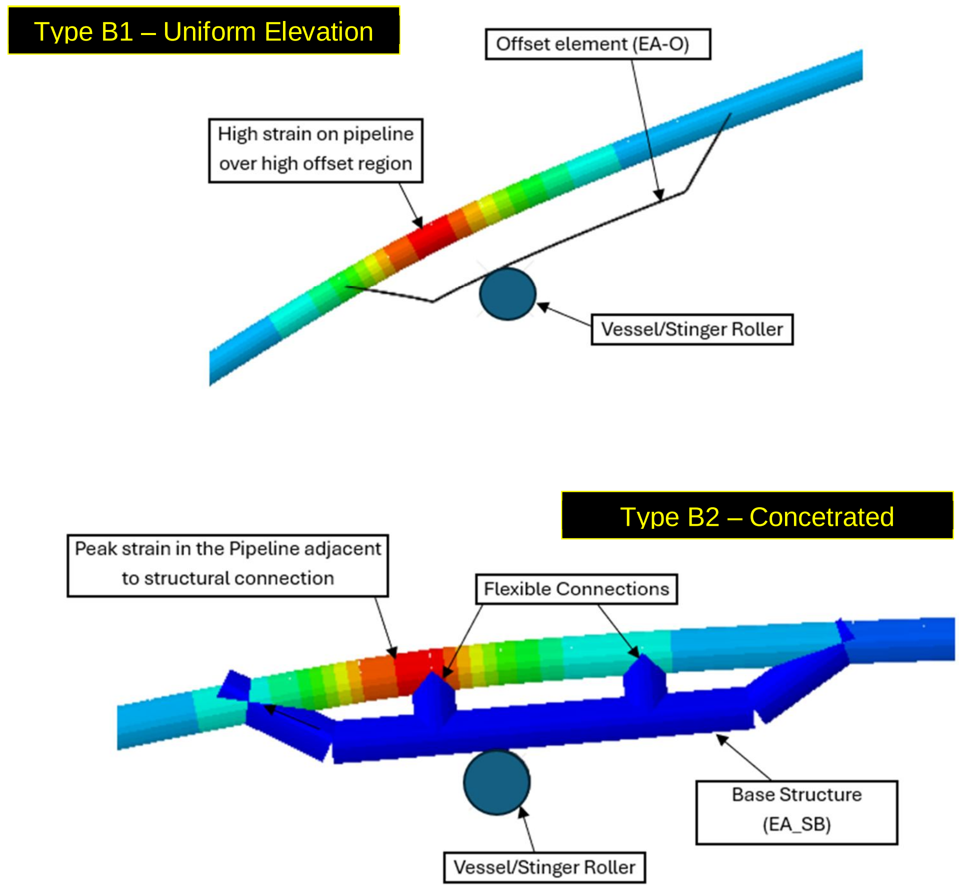

Fig. 15. Example of Type B Mechanical Behaviour

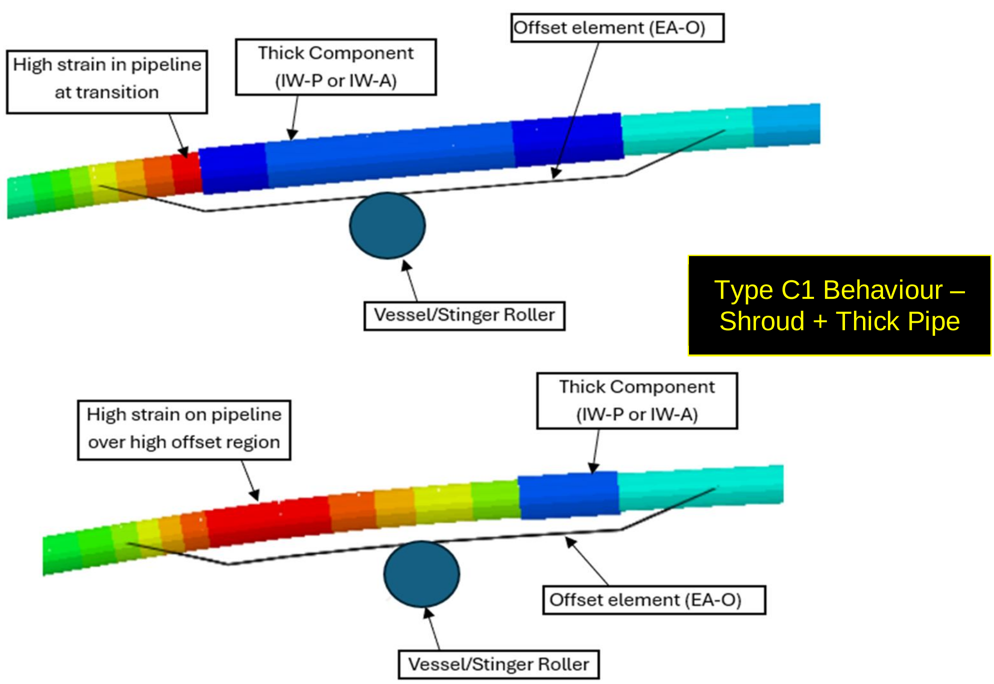

Fig. 16. Example of Type C Mechanical Behaviour

F. *Existing Work and the Gap*

Plain-pipe overbend mechanics are well established. Global installation analysis tools such as PipeLay and OFFPIPE compute catenary moment and curvature; local shell finite element analyses confirm strain at the governing roller position. The strain criteria for deepwater S-lay — including the relationship between stinger radius, overbend strain (e_0 = D/2r), residual curvature, and allowable pipe integrity — are established in [3]. The degree to which the overbend is truly displacement controlled is examined by Jansen[17], who shows that the condition at each stinger roller is partially rather than fully DC, with the degree of partial displacement control varying with roller spacing, pipe diameter, and lay tension; for inline structure passage this PDC degree is expected to change drastically at each roller, an effect he identifies as requiring dedicated Abaqus study. O'Grady and Harte [4] provide a comprehensive local FE assessment framework and show that global tools underestimate overbend strain for smaller-diameter pipes by 10–35%. DNV-ST-F101 [5] codifies DCC strain limits and LCC moment limits for the overbend condition. General pipeline mechanics are covered in [1] and[2]; the foundational textbook treatment of rigid inline sections on the stinger — including the roller offset mechanism and tapered-timber strapping as the established field mitigation — is given in [1].

The industry has addressed inline structure installation engineering at scale across multiple projects, water depths, and installation contractors. Inline structures are routinely deployed on large deepwater projects: Huang et al. [6] describe the installation of over 100 km of flexible flowlines with 24 inline SLEDs and PLETs in water depths to 1,300 m on a single vessel, noting that bending moment at the flowline-to-structure interface is sensitive to layback distance and vertical motion during landing. For rigid pipeline systems, Antani et al. [7] document the J-lay installation of large and heavy PLETs (up to 128 metric tons, 22 m × 11 m) in 4,200 ft water depth in the Gulf of Mexico, demonstrating that inline structure structural engineering requires dedicated FEA across multiple installation load cases. These studies confirm the scale at which inline structures are deployed and that their interaction with the pipeline is a recognised engineering concern. For large-diameter rigid pipeline ILTs with outlet Tees, Kaliyaperumal et al. [16] show that S-lay installation loads must be addressed at the FEED design stage, with overbend and sagbend moments governing the structural configuration of the piping-to-frame connection and the choice between rigid and pinned connection concepts.

The most direct precedent for the problem studied in this paper is the work of Mota [8] on the Lula (TUPI) Pilot Project, which involved the first of its kind in-line PLET installed on an S-lay vessel for an 18-inch rigid pipeline in 2,145 m water depth. This work explicitly confronts the stinger roller passage as a structural design constraint: the component geometry had to respect the tensioner window and enable passage by the rollers. A key engineering concern stated by Mota is the need to avoid excessive bending at valve flange connections during overbend and sagbend passage. The design solution adopted was to leave the hub floating (not rigidly locked to its structure) so it could move freely during stinger passage, with ROV locking performed after the structure reached the seabed. This is a practical engineering response to overbend-induced bending — but the paper stops at the geometric and fitment level and contains no characterization of the strain amplification mechanism in the adjacent pipeline, no quantification of the amplification as a function of component geometry or passage position, and no design criterion for the plain pipeline adjacent to the structure.

A more recent and quantitatively explicit precedent is provided by Bruschi et al.[15], who characterize fatigue damage during deepwater S-lay installation of an inline accessory on the Castorone vessel in the Gulf of Mexico. Their analysis identifies bending strain intensification in the adjacent pipeline concentrated at stinger roller contact points, and reports a peak pipeline strain of 0.83% without mitigation. Two countermeasures are studied: thick-walled transition joints at each component end — equivalent to the Type A stiffness mechanism studied here — and a profiled shroud to redistribute roller contact forces — equivalent to the Type B elevation mechanism. Their combined application reduces peak strain to 0.31%. The Bruschi study is the closest published quantitative precedent to the present work; it demonstrates that targeted mitigation of the strain amplification problem is effective for a specific project geometry, but provides no systematic parametric characterization of how amplification varies with component type, length, elevation, or stinger passage position.

O'Grady and Harte [4] explicitly identify this as an open gap in their Recommendation 3: inline valves, Tees, and end terminations on the stinger are identified as requiring dedicated assessment beyond the plain-pipe framework their paper establishes. Jansen [17] arrives at the same open item from the PDC perspective, explicitly recommending dedicated Abaqus modelling of how inline structure passage changes the degree of partial displacement control at neighboring pipeline sections. The studies cited above confirm that the industry has found practical workarounds — modular assembly, hub floating, buoyancy management, J-lay substitution, and targeted mitigation hardware — but none provides the systematic characterization of overbend strain behaviour as a function of component type and geometry that would underpin a general engineering framework. This paper directly addresses both open recommendations.

II. TRANSITION FROM PIPELINE TO PIPING AND STRUCTURE

A. Thickness of Inline Components – Code Requirements

Subsea inline components —Valves, Tee Forgings, Bulkheads etc — are pressure-containing non-pipe geometries. DNV-ST-F101 [5], which governs pipeline wall thickness and installation strain criteria, applies exclusively to the pipeline. Component bodies with non-circular or complex cross-sections must instead be designed to pressure vessel or piping component codes — typically ASME VIII Division 2 for pressure vessel bodies or ASME B16.34 for valves and fittings. For the same design loading, required wall thickness as per ASME design codes are typically about 2.5 times thicker than DNV requirements. This requires the use of a Tapered thickness transition between the thin and thick sections. Refer Fig. 17 and Fig. 18 for and overview.

The DNV-ST-F101 overbend assessment uses two criteria for the pipeline: the DCC strain criterion (Eq. 5.29, limiting design strain ε_{Rd}) and the LCC moment criterion (Eq. 5.28, limiting bending moment $M \leq M\_char/\gamma c$ where $\gamma c = 0.80$ is a load-side conditional factor). Both criteria apply to the pipeline only. Structural assemblies (EA-S), connection rings (EA-R), and piping components (IW-P, IW-A) are designed by ASME allowable stress criteria — they are load-controlled, not displacement-controlled. This code gap has an operational analogue: Liu et al. [18] show that standard pressure containment specifications for wall thickness transition welds are not adequate for pipes subjected to high longitudinal strain, independently confirming that the thick-to-thin transition is a strain concentration zone under both installation overbend and in-service geohazard loading.

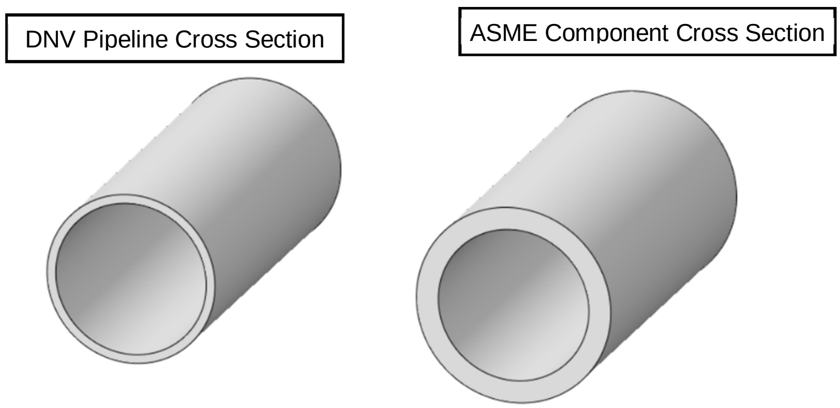

Fig. 17. Cross-section comparison between the DNV 450 pipeline (WT = 21 mm, OD = 406 mm) and the ASME VIII Div.2 DCC-equivalent body (WT = 53 mm, OD = 471 mm) at constant ID = 364 mm. The 2.54× wall thickness increase is entirely outward; it raises the roller contact elevation by 32 mm and increases bending stiffness by approximately 3.2×

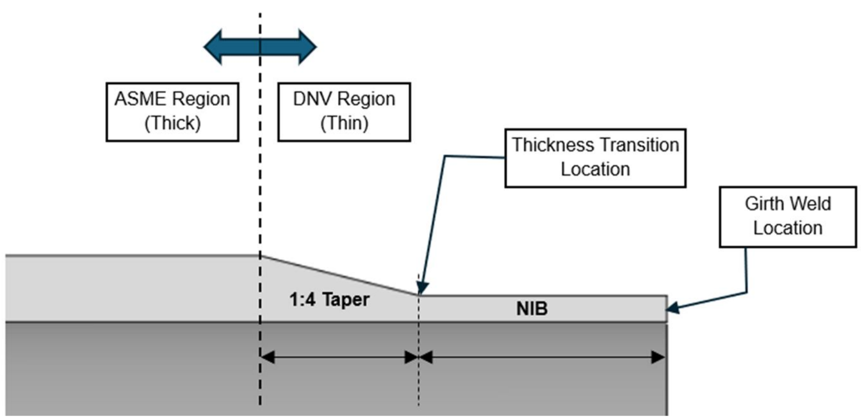

Fig. 18. Tapered transition forging geometry per DNV-ST-F101 §5.6. The NIB ends the girth weld; the code break is at the taper-to-body junction. The 1:4 (minimum) taper is on the outer surface only. The constant bore is maintained throughout for pigging.

The bore must remain constant throughout the inline structure to permit pig passage. For a 16-inch NPS pipeline with ID = 364 mm, the ID is maintained through the taper transition and through the component body. Because the bore does not change, the required wall thickness increase is entirely outward: OD grows outward, and this outward growth has two consequences for the stinger passage problem studied here. First, the increased OD raises the component contact surface above the plain-pipe level at each roller

©IJRASET: All Rights are Reserved

by V = OD_component/2 − OD_pipe/2 (the geometric elevation effect). Second, the thick wall increases bending stiffness EI substantially — for the same ID and material, $EI \propto OD^4 - ID^4$, giving approximately 3.2× the pipeline stiffness for the 16inch pipe considered here (the stiffness discontinuity effect). These two effects are the mechanical origin of the Type A and Type B behaviour studied in this paper and are not optional design choices — they are determined by the governing pressure containment code.

B. Structural Attachment to the Pipeline — Code Requirements

Once a thick-walled component body is designed to ASME VIII, a second code question arises: how does the structural ILT frame connect to the pipeline?

Four approaches are conceptually available

1. Type IW-A: Machine an integral mounting hub on the component separate from the pressure containing wall to weld a structural arrangement (eg: Pipe in Pipe Bulkhead). See Fig. 10.
2. Type IW-A: Machine an integral bolting interface on the component separate from the pressure containing wall. See Fig. 10.
3. Welding to an encircling element.
4. Welding directly to the pipe wall. Both DNV-ST-F101 and ASME B31.8 are explicit on this question.

Approach 1 is the most extensively used in the industry and DNV-ST-F101 provides guidelines for it. Approach 2 has no technical issues, but it provides lesser load transfer capability compared to Approach 1. Approach 3 is technically viable, but there are some challenges in implementing such designs in practice. Refer TABLE III.

The integral girth-welded bulkhead solves the structural attachment problem by making the forging itself a pipeline component. The bulkhead is joined to the pipeline by full-penetration girth butt welds — not fillet welds — with a tapered NIB transition per DNV-ST-F101 §5.6. The structural frame Boss attaches to the bulkhead OD in the ASME VIII Div. 2 zone, not to the pipeline pressure wall. The pipeline-side welds are covered by DNV-ST-F101 Table 11-1 workmanship criteria as standard. DNV-ST-F101 § 13.6.5 formally classifies the bulkhead as a pipeline component and defines the code split: the weld-end zones operate under DNV-ST-F101, the centre body under ASME VIII Div. 2.

For new-build subsea ILT/PLET components fabricated onshore, the integral girth-welded bulkhead is the engineering standard: it gives designable fatigue performance through taper geometry, a single weld toe crack location, standard weld acceptance criteria, and full ILI inspectability. The welded sleeve is a repair and remediation geometry — its use in new-build requires a full ECA before fabrication and leaves the assembly with higher residual stress, more crack locations, and reduced inspectability compared to an integral solution.

TABLE III. INTEGRITY ISSUES SPECIFIC TO THE WELDED SLEEVE (FILLET GIRTH WELD) CONNECTION.

Issue	Detail
Crack locations	Three simultaneous: (1) weld toe — carrier pipe wall; (2) weld root — weld throat; (3) sleeve-end lack-of-fusion. Each requires separate ECA with different governing loads.
Governing S-lay load	Axial lay tension governs at the weld toe. Internal pressure alone closes the weld toe crack (moment is negative, Semiga et al. 2016). Lay tension oscillation from vessel heave is the fatigue driver.
Residual stress	750–860 MPa hoop at weld toe for X80 carrier / Q345B sleeve (Zhang et al. 2021). This eliminates the R-ratio benefit — the crack-tip stress remains tensile throughout the full fatigue cycle.
Sleeve material constraint	Must be LOWER strength than carrier pipe. Upgrading sleeve to match carrier grade increases residual stress and crack risk. Higher-strength steels sustain larger residual stresses during cooling.
Fillet weld size	Minimum 1.4T per ASME B31.8 (T = carrier pipe WT). Preferred 2.0T or larger. Reducing fillet size to save welding is prohibited — directly increases stress and crack risk.

Annular gap load case	If carrier pipe is penetrated or through-cracked, the annulus between sleeve bore and pipe OD pressurises. This reverses the loading on the lack-of-fusion crack — unique to this geometry.
Weld acceptance criteria	None in DNV-ST-F101 (Table 11-1 covers butt welds only). ECA to BS 7910:2013 using Semiga et al. (2016) SIF solutions is mandatory before fabrication. No prescriptive dimensional limits exist.
ILI inspectability	Weld root crack in annular gap is not accessible to standard MFL or conventional ILI tools. Only specialised PAUT from the outer surface can reach it. Root and lack-of-fusion are hidden at fabrication.

III.PHILOSOPHY AND SCOPE OF WORK

A. Design Philosophy: AI-Assisted Conceptual Engineering

Inline Component assemblies, including Subsea ILT and PLETs for a given piping layout can be configured in a large number of ways. The choice of IW/EA component types, their mechanical connection arrangement, the structural geometry of any base structure, and the position of the assembly along the stinger all influence the strain response of the adjacent pipeline during S-Lay installation. Exhaustive concept screening by full finite element analysis is impractical under fast-track project timelines, where project teams must often adapt previously successful configurations to new conditions with limited opportunity for systematic optimization.

In this context, AI-assisted conceptual engineering offers a practical path forward. An AI collaborator equipped with design intuition — a structured, quantitative understanding of how each component type and geometric parameter governs the overbend strain response — can propose initial assembly configurations for human-expert review, identify the dominant mechanical behaviour type before any analysis is performed, and guide the analyst toward the most sensitive design parameters. This reframes the engineer's role from exhaustive screener to validator and decision-maker, enabling faster concept development and more systematic coverage of the design space.

B. The Developmental Programme

Realizing this capability requires the sequential development of seven engineering competencies, each building on its predecessor. The programme is summarized in TABLE IV. Step 1 – Component Taxonomy, and Step 2 (partial) - Design Intuition — is addressed directly by the present paper; Steps 2 (remaining) through 7 define the roadmap for subsequent work.

TABLE IV. SEVEN-STEP AI-ASSISTED CONCEPTUAL ENGINEERING DEVELOPMENT PROGRAMME

Step	Capability	Objective	Scope
1	Component Taxonomy	Identify the fundamental components of the assembly and classify them with ID tags for consistent identification	**This Paper**
2	Design Intuition	Characterise strain amplification mechanisms for each IW/EA component type as a function of geometry, length, elevation offset and attachment stiffness. Components can be classified into two groups as below	**This Paper**
		1) Type A1, B1 and C1: Applicable for IW-P, IW-A, EA-O	
		2) Type A2, B2 and C2: Applicable for EA-BS, EA-TS, EA-R	**Future Work**
3	Intuitive Assembly	Predict dominant mechanical behaviour(s) type (A, B, or C) for a given assembly configuration before analysis. Translate component-level intuition into assembly-level design judgement.	**Future Work**
4	Simplified Analysis	Develop reduced-order models for rapid parametric sensitivity	Future Work

Step	Capability	Objective	Scope
		screening without full Abaqus execution. Enable AI-driven iteration at concept stage.	
5	Design Code Assessment	Automate DNV-ST-F101 and ASME VIII capacity checks against computed demands. Integrate code compliance as a primary concept filter.	Future Work
6	Iterative Analysis	Closed-loop automated parametric workflow combining simplified models, code checks, and structured result interpretation with minimal manual intervention.	Future Work
7	Configuration Optimization	Identify governing parameters and systematically adjust toward minimum peak strain configurations within applicable code limits.	Future Work

C. Scope of the Present Paper

The present paper addresses Step 1 and Step 2 (partially) of the program above. Through parametric finite element analyses using Abaqus, incorporating stinger-pipeline contact modelling under representative S-Lay loading conditions, it characterizes the isolated mechanical behaviour of each inline component type (Types A1, B1 and C) as a function of the key geometric parameters governing its strain response. The results identify the dominant amplification mechanisms, the direction and relative magnitude of the governing parameter effects, and the conditions under which peak strain transfers between pipeline locations. The findings, along with future work on Types A2, B2 and C2 will form the design intuition upon which Steps 3 through 7 will be built.

D. Parametric Study Plan

TABLE V summarises the four component types studied, the physical phenomena investigated for each, and the geometric parameters varied in the parametric runs. The effect of stinger configuration (radius R, top tension T) on these behaviour patterns is addressed separately in Section IV.

TABLE V. Parametric Study Plan — Component Types, Phenomena, and Parameters

Type	IW/EA Class	Phenomena Investigated	Parameters Varied
Type A1 *Thick Pipe with Transition*	**IW-A / IW-P**	– Effect of taper angle (transition slope) on strain concentration at the NIB-to-body junction – Strain gradient across the tapered transition zone	– Transition slope (L:1 ratio)
Type A1 *Thick Pipe (Body only)*	**IW-A / IW-P**	– Effect of wall thickness ratio on strain amplification in adjacent pipe – Effect of thick section length on strain amplification and distribution – Effect of spacing between successive thick components – Position sensitivity: effect of component location along stinger	– Wall thickness ratio T/t – Thick section length L/D – Inter-component spacing
Type B1 *Offset Element*	**EA-O**	– Effect of offset magnitude (depth) on local pipeline curvature – Effect of offset length on strain gradient and peak location – Effect of taper slope at offset transitions – Strain variation along component length – Position sensitivity: effect of component location along	– Offset depth V/D – Offset length – Taper slope

Type	IW/EA Class	Phenomena Investigated	Parameters Varied
		stinger	
Type C1 *Combined: Offset + Thick Pipe*	**EA-O + IW-A / IW-P**	– Combined effect of elevation offset and stiffness discontinuity on peak strain – Effect of thick section location relative to offset centre – Strain distribution along assembly length	– Offset depth – Thick section wall thickness and length – Thick section location

E. Analysis Series Summary

The parametric study is conducted as a sequence of five analysis series, each introducing one additional level of geometric complexity relative to the plain pipe baseline. This progression allows each effect to be isolated cleanly before combinations are introduced. TABLE VI summarises the series and their objectives.

TABLE VI. ANALYSIS SERIES — PROGRESSION FROM BENCHMARK TO FULL ASSEMBLY

Series	Analysis Description	Mechanical Type	Aim
1	Plain Pipe — S-Lay overbend, no inline component	—	Benchmark: validate against analytical strain solution and compare with published literature
2	Pipelay with tapered transition elements	**Type A1**	Parametric study of taper slope variation effect
3	Pipelay with thick piping components	**Type A1**	Parametric study of wall thickness, length, and spacing effects
4	Pipelay with offset elements	**Type B1**	Parametric study of elevation offset geometry effects
5	Pipelay with combined offset + thick pipe elements	**Type C1**	Parametric study of combined stiffness and elevation effects

IV. STATE OF ART REVIEW : FEA OF S-LAY ANALYSIS AND PLAIN PIPE BEHAVIOUR

A. Standard Practices for S-Lay Analysis by FEA

In industry practice, stress and strain analysis of pipelay by FEA is performed primarily using beam element models of the pipeline, with geometric and material nonlinearity and full pipe-to-roller and pipe-to-seabed contact interaction. Specialized pipelay programs such as Orcaflex and Offpipe implement these fundamental FEA methods through interfaces optimized for pipeline analysis. When studying non-pipeline components such as ILT assemblies, or when components must be modelled in greater geometric detail (e.g. using shell or solid elements), general-purpose FEA programs such as Abaqus offer significant advantages.

The Abaqus beam-element approach with discrete rigid roller contact is now well established for S-Lay overbend strain analysis. Three key studies directly underpin the modelling approach adopted in the present paper and are summarized in TABLE VII.

TABLE VII. KEY PRIOR STUDIES SUPPORTING THE FEA APPROACH USED IN THIS PAPER

Reference	FEA Approach	Key Findings	Relevance to This Study
Yun et al.[19]	Abaqus/Standard beam elements; frictionless rigid roller surfaces; one- and two-roller configurations	Roller spacing and lay tension govern curvature concentration at each roller. Loading history (sliding through vs. draping) is essential for accurate strains, particularly at	*Validates quasi-static passage simulation; establishes roller model benchmark for this study*

Reference	FEA Approach	Key Findings	Relevance to This Study
		high lay tension where inter-roller spans partially straighten.	
Ivić et al. [11]	Abaqus beam elements; frictional contact tensioner model; contact with rollers and seabed	Frictional contact tensioner produces near-perfect match with Offpipe (industry standard). Confirms that beam-element Abaqus approach accurately reproduces S-Lay global behaviour.	*Validates beam-element modelling approach and Abaqus-to-Offpipe agreement used here*
Ai et al. [20]	Lumped-mass pipeline model; discrete roller contact; validated against ORCAFLEX	Static-dynamic overbend strain difference is only 1.3%. Overbend strains are controlled by stinger radius, not vessel dynamics. Confirms displacement-controlled nature of overbend.	*Justifies quasi-static approach; confirms DC condition assumed in parametric study*

B. Three Phases of Stinger Passage

Yun et al. [19] demonstrated that as a pipe section travels from the vessel through the stinger and into open water, it experiences three mechanically distinct phases. Understanding these phases is essential for correct interpretation of parametric results: the governing phase for plain pipe is Phase 1, but this may differ for inline components and requires verification. Additionally, a moving pipeline model — in which the pipe slides progressively through the rollers rather than being draped statically — is necessary to capture the full loading and unloading history. TABLE VIII summarises the three phases.

TABLE VIII. THREE PHASES OF STINGER PASSAGE (AFTER YUN ET AL. [19])

Phase	Name and Location	Physical Behaviour	Strain Implication
1	Plastic Bending *(Tensioner → First few rollers)*	Initially straight, stress-free pipe passes through tensioner and onto first roller boxes. Pipe is plastically bent to a curvature slightly exceeding the local stinger curvature due to strain concentration at roller contact. Typically completes within the first two roller boxes.	PEAK STRAINS — governs design. Phase 1 produces the highest strains for plain pipe (Yun et al. [19]). Applicability to inline components to be confirmed by this study.
2	Elastic Bending *(Stinger mid-rollers)*	Pipe slides over remaining mid-stinger rollers in a repeating bending-unloading cycle. Deformation is elastic — moment-curvature relationship is linear, offset by residual plastic curvature from Phase 1. Curvature peaks at each roller, reaches minimum at mid-span.	Oscillating strain — magnitude governed by roller spacing and lay tension. Strain range is lower than Phase 1 for plain pipe.
3	Free Departure *(Beyond last roller)*	Pipe section slides off the last stinger roller and is no longer stinger-supported. Numerical results indicate the pipe can be severely bent at departure.	ADVERSE — severe bending at departure is an undesirable scenario. Departure strains are monitored but do not typically govern for plain pipe.

C. Single Roller vs Multi-Roller Modelling

A typical roller box consists of multiple rollers assembled on a frame structure that pivots about a central hinge. For FEA, the question arises whether to model the full roller box geometry or to represent it as a single roller contact point. Yun et al. [19] investigated this directly by comparing one-roller and two-roller configurations. The primary difference lies in the severity and distribution of deformation: the one-roller model concentrates bending at a single contact location, producing more severe local strain. The quantitative comparison is given in TABLE IX.

TABLE IX. ONE-ROLLER VS TWO-ROLLER MODEL COMPARISON (AFTER YUN ET AL.[19])

Parameter	One-Roller Model	Two-Roller Model	Implication
Strain range (total)	0.111%	0.047%	~2.4× higher in one-roller model
Stress range	227 MPa	96 MPa	~2.4× higher in one-roller model
Extensional (axial) strain	0.204%	0.174%	~10% difference — plastic bending in Phase 1
Maximum bending moment	658kNm	633kNm	~5% difference only
Minimum bending moment	171kNm	424kNm	~60% lower — greater elastic unloading range
Bending/curvature variation	High — concentrated at single contact	Lower — distributed across two contacts	One-roller overestimates strain oscillation
Model adopted for this study	**Single roller**	—	*Aim is study of relative behaviour with parameter variation, not absolute strain accuracy*

† *For the present parametric study, the single-roller model is adopted. Since the objective is to characterise relative strain behaviour as a function of component geometry — not to compute absolute strain values — the consistent use of single-roller contact across all runs preserves comparability while the absolute values remain conservative.*

V. ABAQUS S-LAY ANALYSIS MODEL AND METHODOLOGY

A. Parts

Abaqus model consists mainly of 2 parts

- Pipeline: Modelled with beam elements. The model is long enough to cover the entire length of the stinger + vessel rollers + extra length to suit translation. Modelled with B31 elements. Mesh size = 2 x OD (In similar range of mesh size followed by Orcaflex [21]). Refer Fig. 19.
- Rollers: Rigid surface of 300mm Radius modelled with R3D4 elements. This radius is selected to be similar to typical stinger rollers. Refer Fig. 20.

For EA-O consideration, an additional part is modelled

- Shroud: Modelled with Surface element. Refer Fig. 21.

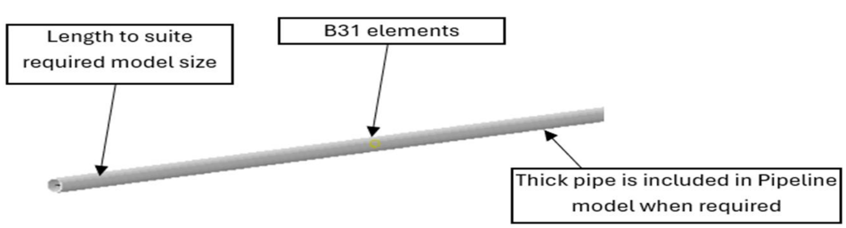

Fig. 19. Pipeline Part (Variable geometry)

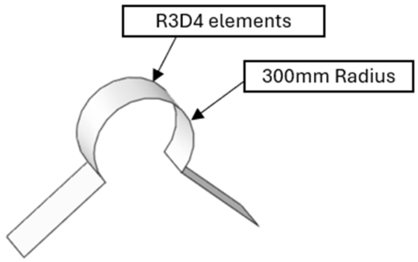

Fig. 20. Roller Part

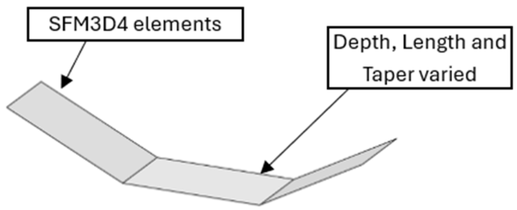

Fig. 21. Shroud Part (Variable geometry)

B. Stinger and Firing Line Modelling

Stinger and Firing line are modelled by fixing the rollers at regular intervals along the hypothetical radius of the Stinger and the straight level of the firing line. Refer Fig. 22. Rollers are spaced out at length of 9m c/c. Referring to Section 1, this is based on typical roller spacing in vessels, more towards the conservative side.

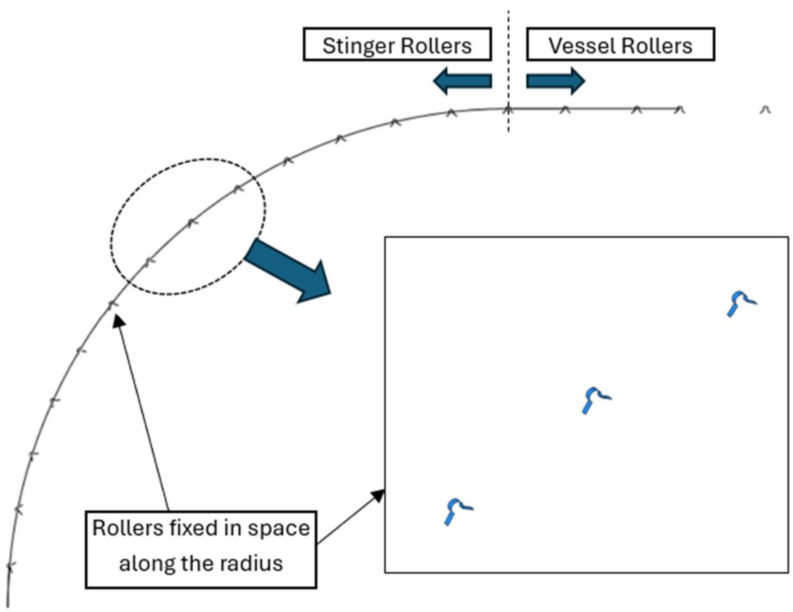

Fig. 22. Stinger and Firing line Model

International Journal for Research in Applied Science & Engineering Technology (IJRASET)
ISSN: 2321-9653; IC Value: 45.98; SJ Impact Factor: 7.538
Volume 14 Issue VII July 2026- Available at www.ijraset.com

C. Assembly

Pipeline and Roller parts are placed in the Assembly as shown in Fig. 23. Pipeline Part is placed over the Vessel rollers at start. Contact interactions are defined between Pipeline outer surface and Roller surfaces.

Fig. 24 shows modelling of Shroud to pipeline and Shroud to Roller interaction. Shroud top surface (facing the pipeline) is tied to the Pipeline above. Contact interaction is defined between Shroud bottom surface and Roller top surfaces.

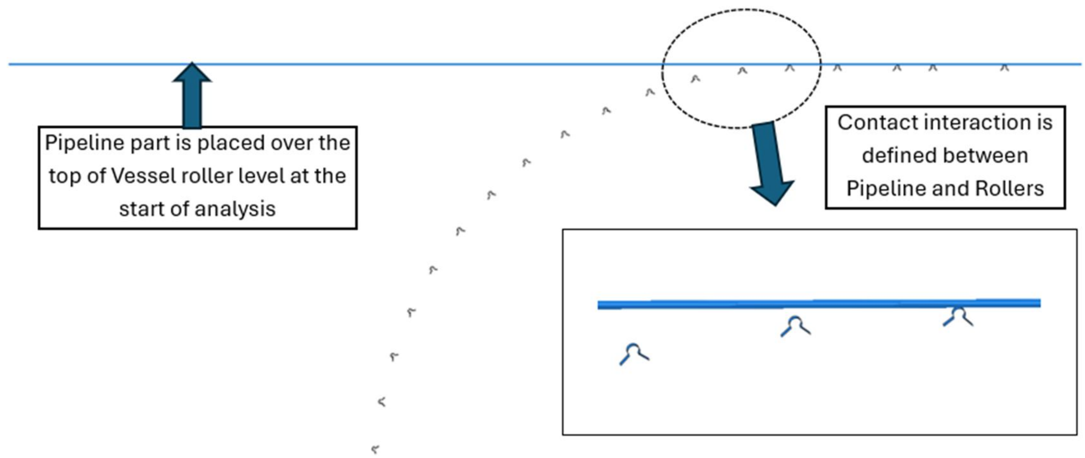

Fig. 23. Pipeline – Stinger Assembly

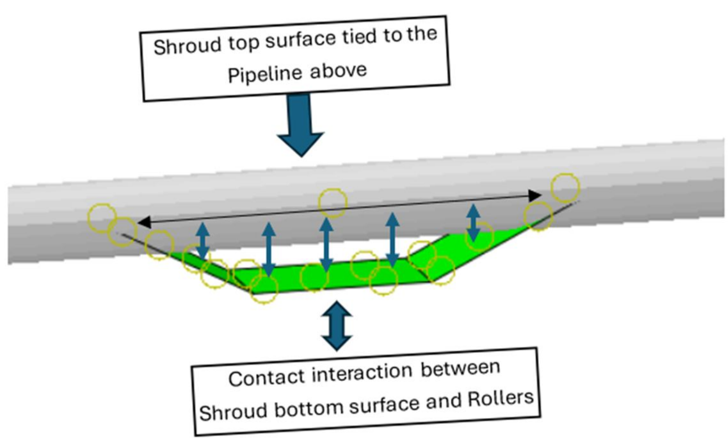

Fig. 24. Pipeline – Shroud Assembly

D. Loads, Imposed Displacements and Boundary Conditions

Analysis is conducted in 5 steps

1) Apply a pretension at the catenary end node to stabilize the model through tension, while fixing the vessel end.
2) Apply rotation at catenary end node to bend the pipeline along the stinge
3) Apply gravity
4) Apply pipelay tension at the catenary end
5) Apply translation at the vessel end to simulate the pipelay by sliding the pipeline over the rollers

©IJRASET: All Rights are Reserved | SJ Impact Factor 7.538 | ISRA Journal Impact Factor 7.894 |

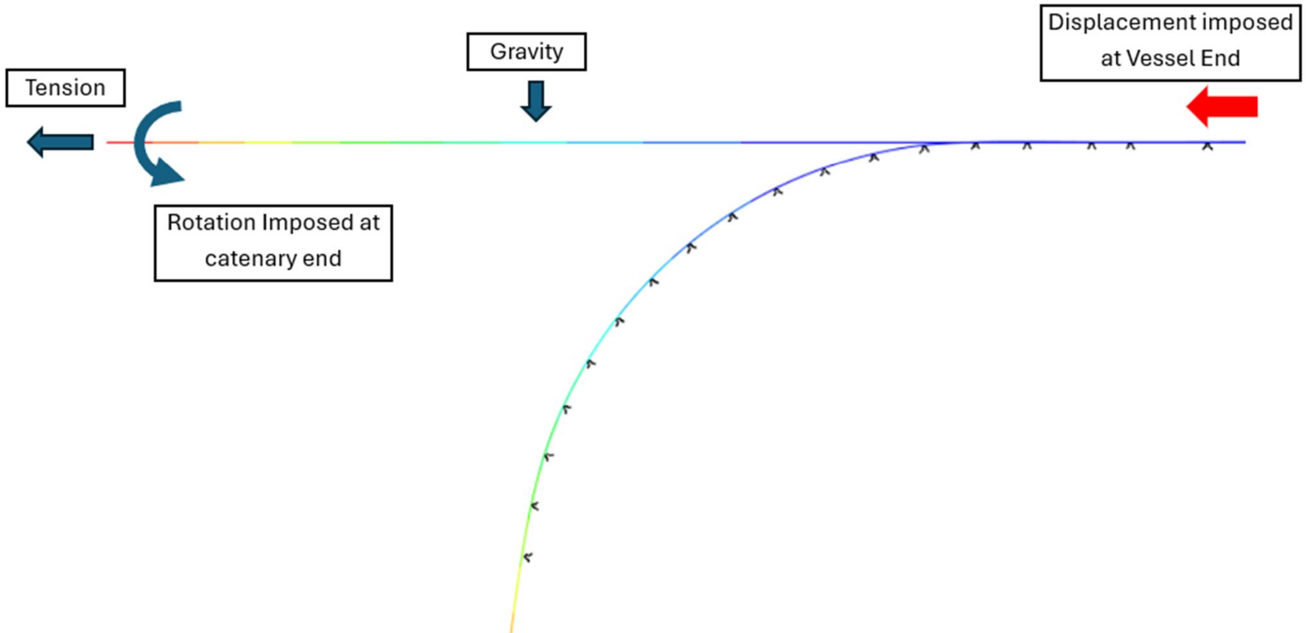

Fig. 25. Analysis Methodology

VI. PARAMETRIC EVALUATION: PLAIN PIPELINE BEHAVIOUR

A. Study 1 Detail

This study correspond to Series 1 in TABLE VI — the plain pipeline benchmark. The aim is to validate the Abaqus overbend model against analytical strain and to establish a baseline against which subsequent inline component studies (Series 2–5) are compared. Two study groups are reported in this section.

- Study 1 examines the effect of stinger configuration (Configs A, B, and C, as defined in TABLE X) on peak strain for a fixed 16in pipeline, benchmarked against the analytical curvature-based strain estimate $\varepsilon = D/2R$.
- Study 2 examines the effect of pipe diameter and applied tension on Phase 1 strain, at a fixed stinger radius of R = 70 m.

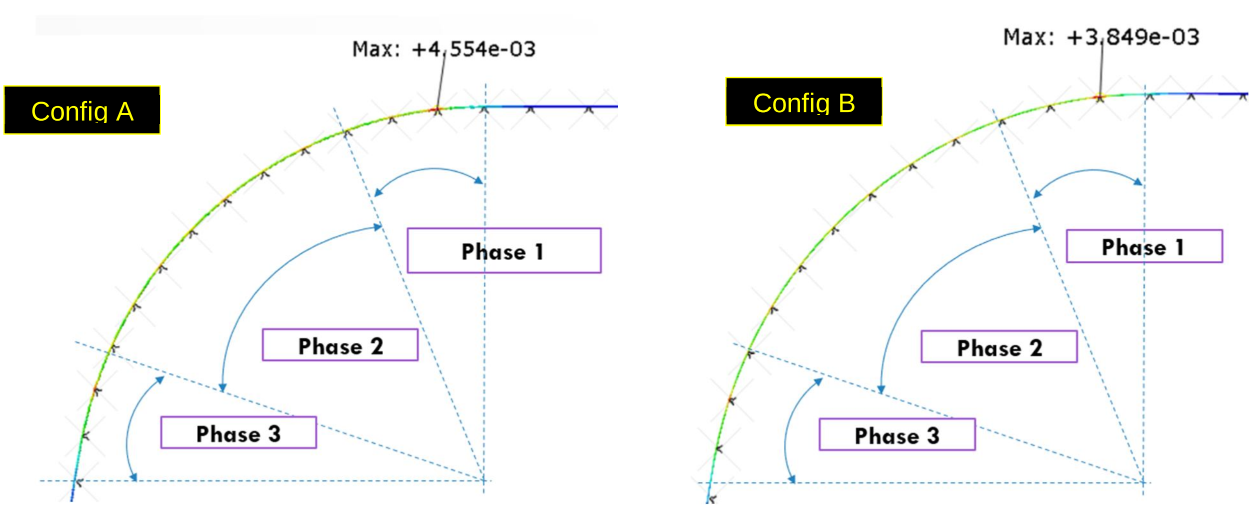

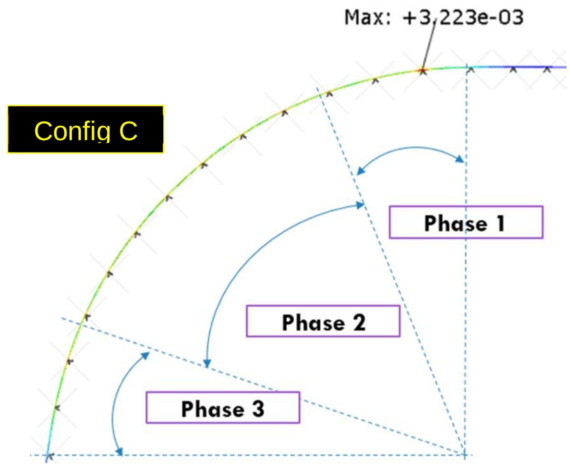

Fig. 26. Nominal Strain and Deformed Model Plot

TABLE X and TABLE XI summarises peak strain for the 16 in pipeline (406 mm OD × 21 mm WT) under each of the three stinger configurations considered, which occurs for during Phase 1.

TABLE X. STUDY 1 RESULTS — PEAK STRAIN BY STINGER CONFIGURATION

Configuration	Tension	Pipeline	Max Strain	Governing Phase
Config A (R = 70 m)	120 MT	16 in (406 mm OD × 21 mm WT)	**0.46%**	Phase 1
Config B (R = 85 m)	120 MT	16 in (406 mm OD × 21 mm WT)	**0.38%**	Phase 1
Config C (R = 105 m)	120 MT	16 in (406 mm OD × 21 mm WT)	**0.32%**	Phase 1

TABLE XI. STUDY 2 — EFFECT OF PIPE DIAMETER AND TENSION ON PHASE 1 STRAIN (R = 70 M)

Pipe OD × WT	Tension	FEA Strain (Phase 1)	Analytical Strain (D/2R)	Difference
6 in (168 mm OD × 21 mm WT)	0 MT	**0.13%**	0.12%	+8%
6 in (168 mm OD × 21 mm WT)	**100 MT**	**0.29%**	—	tension case
16 in (406 mm OD × 21 mm WT)	0 MT	**0.33%**	0.29%	+14%
16 in (406 mm OD × 21 mm WT)	**100 MT**	**0.42%**	—	tension case
20 in (508 mm OD × 21 mm WT)	0 MT	**0.42%**	0.36%	+17%
20 in (508 mm OD × 21 mm WT)	**100 MT**	**0.54%**	—	tension case

B. Trend Visualisation

Tabulated results in previous subsections are reproduced below as trend plots, allowing the direction and rate of change of strain with each governing parameter to be assessed visually.

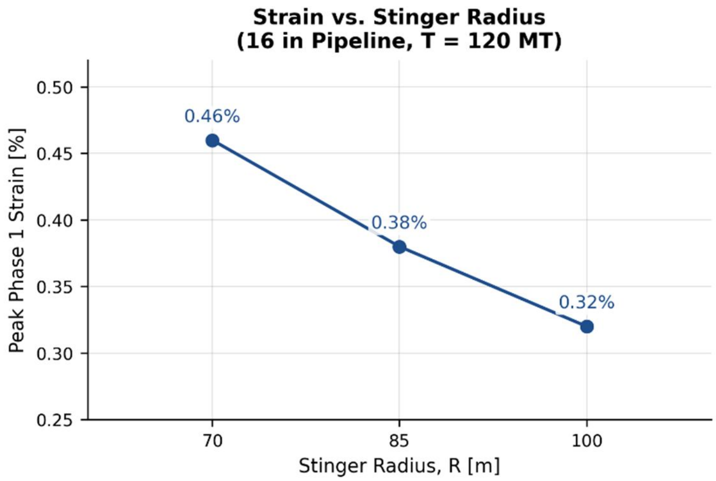

Fig. 27. Peak Phase 1 strain decreases monotonically with increasing stinger radius.

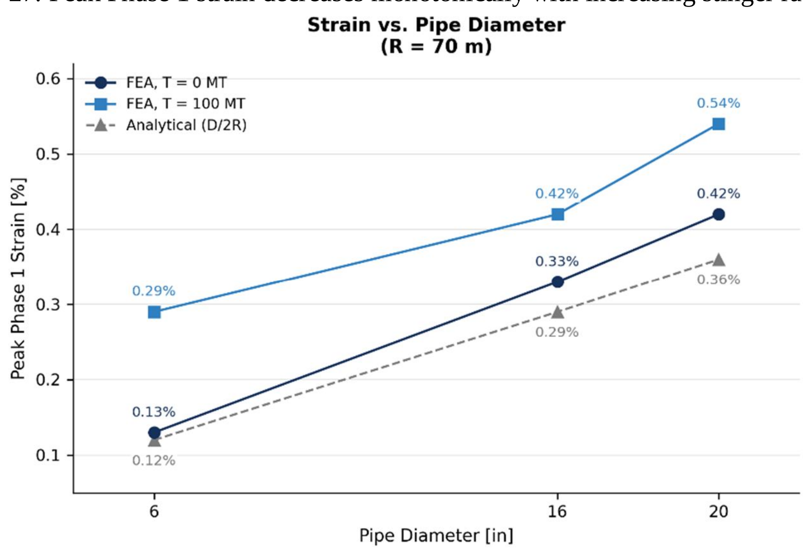

Fig. 28. Peak Phase 1 strain increases with both pipe diameter and applied tension; the FEA-to-analytical gap widens with diameter.

C. Key Insights

- The Phase 1 high-strain effect identified by Yun et al.[19] for plain pipe is confirmed in the present Abaqus model: Phase 1 governs peak strain in all cases tested.
- For the no-tension case (Study Group 1), FEA strain closely matches the analytical estimate ε = D/2R, with the difference increasing modestly with pipe diameter (+8% at 6 in, rising to +17% at 20 in).
- Applied tension increases peak strain substantially relative to the no-tension case across all diameters tested.
- Increasing stinger radius (R = 70 → 85 → 105 m) reduces peak strain monotonically, from 0.46% to 0.38% to 0.32% — consistent with the expected inverse relationship between stinger radius and overbend curvature.

VII. PARAMETRIC EVALUATION: TYPE A1 BEHAVIOUR – TAPERED TRANSITIONS

A. Study Detail

Studies done in this section correspond to Series 2 in TABLE VI — pipelay with tapered transition elements. Inline components (IW-P and IW-A) require a tapered transition at each end between the component wall thickness and the pipeline wall thickness.

DNV-ST-F101 §5.6 stipulates a minimum taper slope of 1:4 on the outer surface. This study evaluates whether the DNV minimum slope is the design optimum from an overbend strain perspective, and whether shallower tapers incur a significant strain penalty. Refer TABLE XII for model details.

TABLE XII. **PARAMETERS:** EFFECT OF TAPER RATIO ON PEAK PIPELINE STRAIN.

Parameter	Value
Pipeline	406.4 mm OD (16 in) × 21 mm WT
Thick section wall thickness	65 mm (≈3.1× pipeline WT)
Thick section length	1000 mm (~2.5×OD)
Taper ratios studied	1:4 (L≈0.43D) — 1:16 (L≈1.7D) — 1:64 (L≈6.9D)†
Stinger configurations	R = 70 m (Config A) — R = 85 m (Config B) — R = 100 m (Config C)
Top tension	120 MT
Mesh at transition	Very fine: element length = 0.25D (results higher than standard mesh; relative trends valid)
Code limit (taper)	Minimum slope 1:4 outer surface (DNV-ST-F101 §5.6)

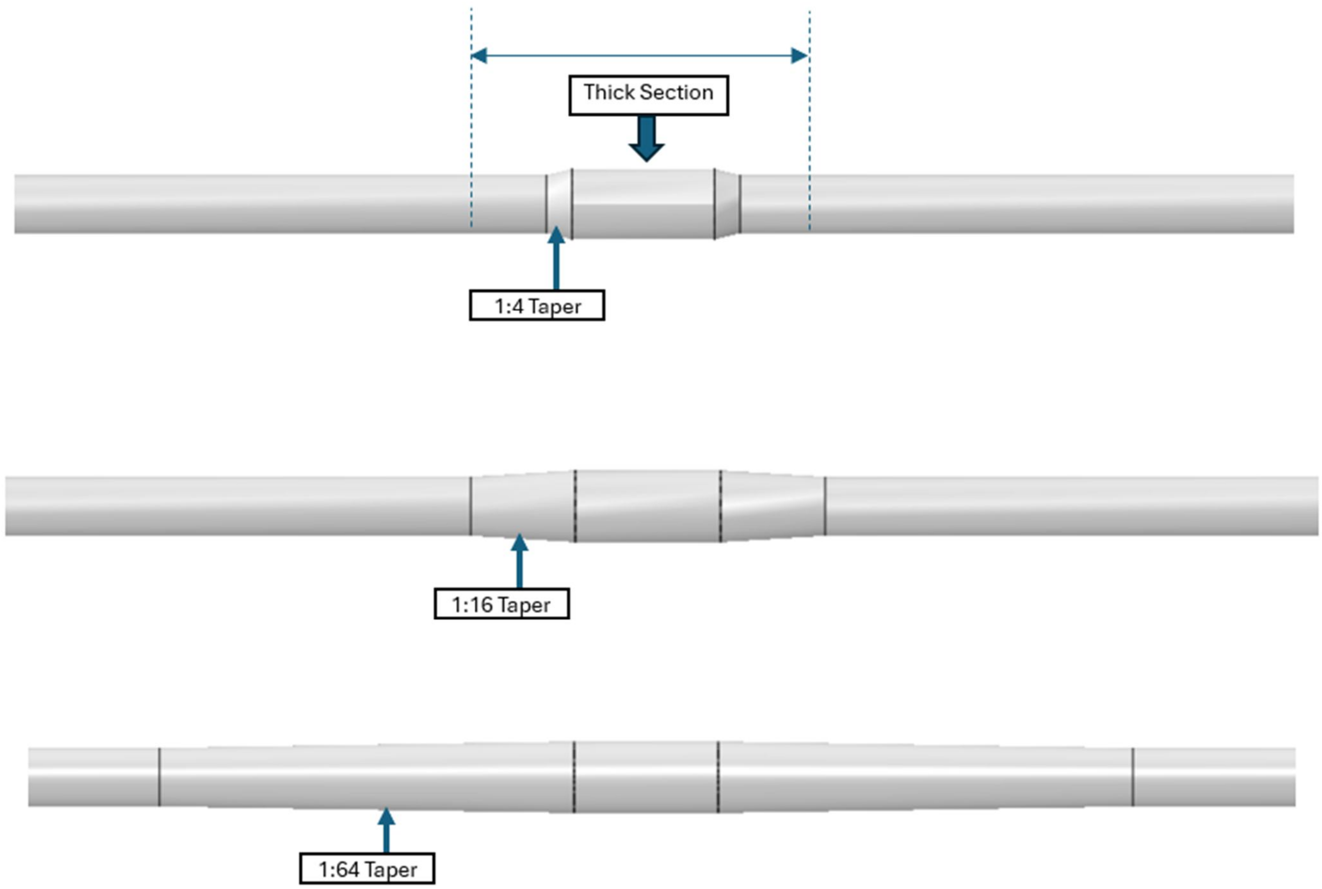

Fig. 29. Tapered Transition Geometries Studied

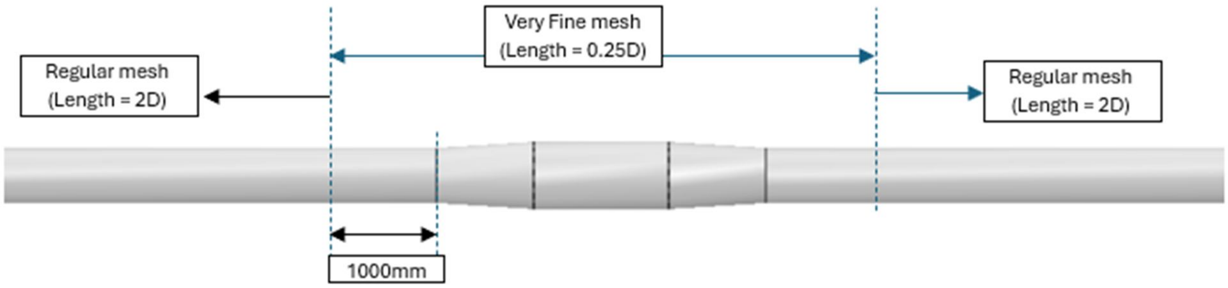

Fig. 30. Mesh Refinement

B. Input Cases

Nine cases are studied: 3 taper ratios × 3 stinger configurations. TABLE XIII presents the full case matrix.

TABLE XIII. INPUT CASE MATRIX — TAPER RATIO × STINGER CONFIGURATION (9 CASES TOTAL)

Stinger Config	Taper 1:4 (L≈0.43D)	Taper 1:16 (L≈1.7D)	Taper 1:64 (L≈6.9D)	Fixed Parameters
R=70m (Config A)	*Case 1*	*Case 2*	*Case 3*	WT=65mm, L=1000mm T=120MT
R=85m (Config B)	*Case 4*	*Case 5*	*Case 6*	
R=100m (Config C)	*Case 7*	*Case 8*	*Case 9*	

C. Results — Peak Pipeline Strain

Peak strain occurs consistently at the pipeline element immediately outside the taper zone (straight pipe to transition junction), when the thick section sits over a stinger roller. TABLE XIV presents results colour-graded against the DNV 2% limit. Fig. 33 shows the hockey-stick trend — flat within the code-compliant zone (1:4–1:16), step increase at 1:64.

TABLE XIV. PEAK PIPELINE STRAIN — EFFECT OF TAPER RATIO (COLOUR-GRADED VS DNV 2% LIMIT)

Stinger Radius	Taper 1:4 (L≈0.43D)	Taper 1:16 (L≈1.7D)	Taper 1:64 (L≈6.9D)	Location
R=70m (Config A)	1.14%	1.19%	2.58%	*Straight pipe / Transition Jn.*
R=85m (Config B)	0.91%	0.94%	1.27%	*Straight pipe / Transition Jn.*
R=100m (Config C)	0.65%	0.69%	0.87%	*Straight pipe / Transition Jn.*

Red ≥2.0% (exceeds DNV limit) • Orange 1.5–2.0% • Amber 1.0–1.5% • Green <1.0%

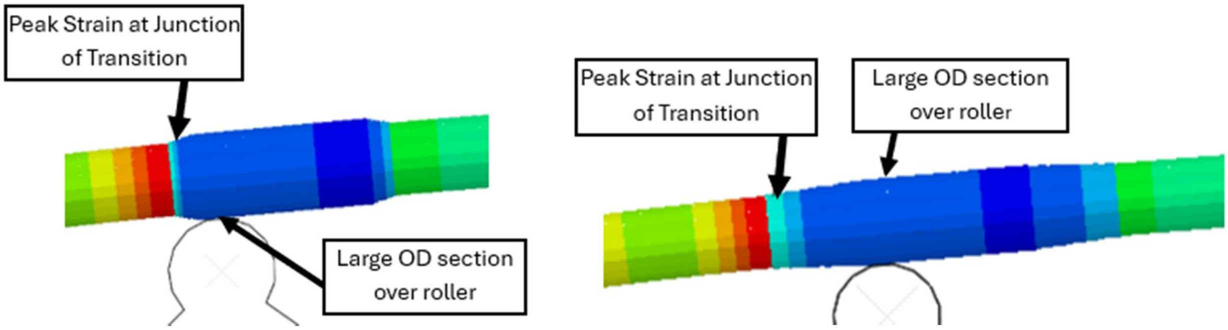

Fig. 31. Typical Peak Strain Characteristics – 1:4 and 1:16 Transitions

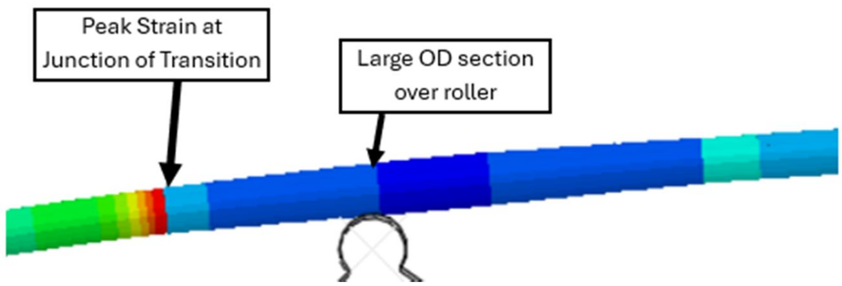

Fig. 32. Typical Peak Strain Characteristics – 1:64 Transition

Refer Fig. 31 and Fig. 32 for Strain plot results one of the cases (Radius = 85m). It can be observed that peak strain occurs at the junction of the straight pipe and transition. And it occurs while the large OD section is over the rollers.

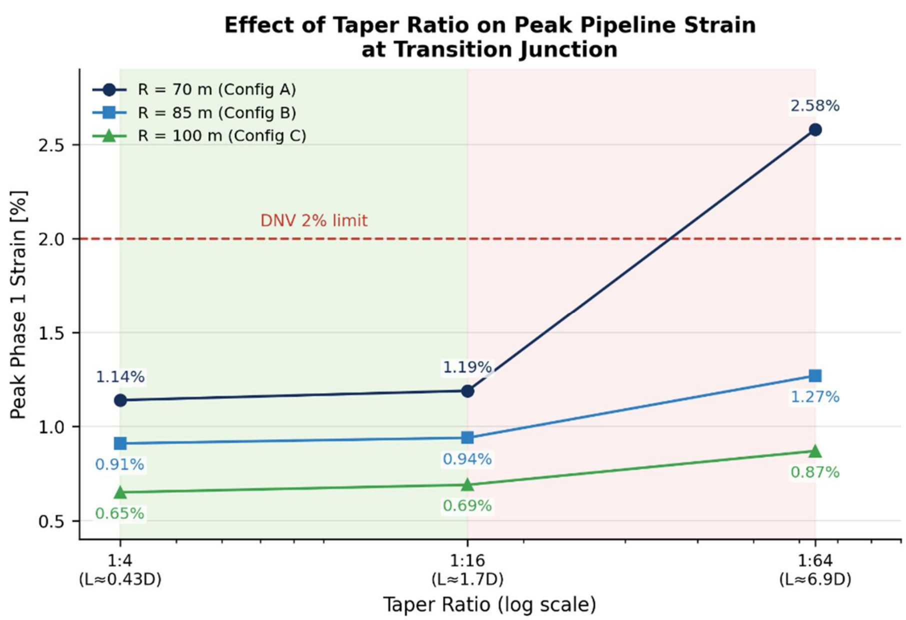

Fig. 33. Strain vs taper ratio (log scale). Green zone = DNV-compliant range (1:4–1:16): strain is nearly flat. Step-change at 1:64 exceeds DNV 2% limit at R=70m.

D. Results — Peak Bending Moment

Peak bending moment occurs in the body of the thick section (not at the transition). The same hockey-stick pattern is observed. See TABLE XV and Fig. 34 present results.

TABLE XV. EFFECT OF TAPER RATIO ON PEAK BENDING MOMENT

Stinger radius	Taper 1:4 (L≈0.43D)	Taper 1:16 (L≈1.7D)	Taper 1:64 (L≈6.9D)	Location
R = 70 m	1413 kNm	1478 kNm	1720 kNm	Body of the thick section
R = 85 m	1390 kNm	1471 kNm	1711 kNm	
R = 100 m	1330 kNm	1384 kNm	1659 kNm	

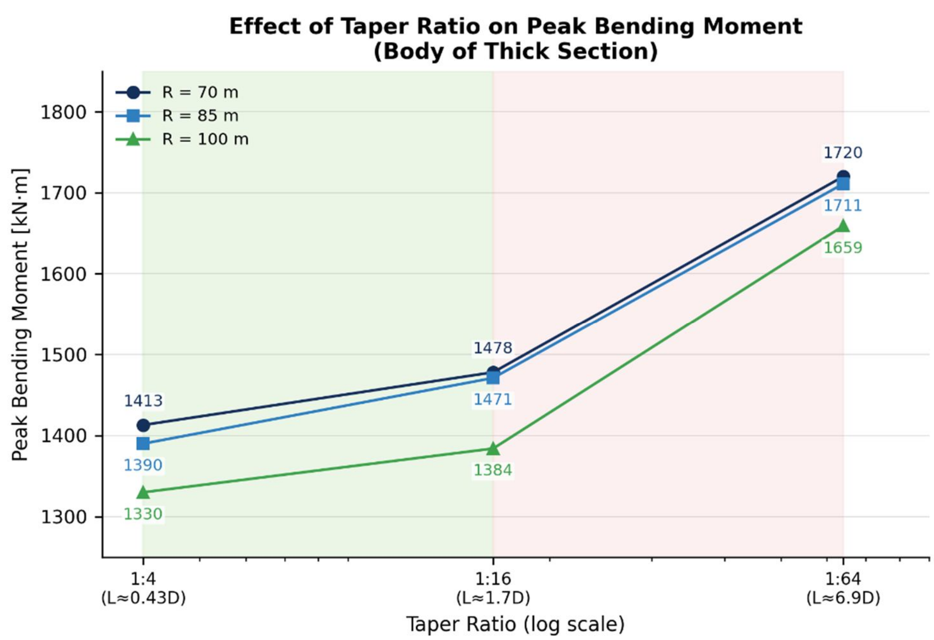

Fig. 34. Bending moment vs taper ratio. Same hockey-stick pattern: flat within code-compliant zone, +18–22% jump at 1:64.

E. Design Insights

TABLE XVI. DESIGN INSIGHTS — TYPE A1 TAPER RATIO STUDY

Insight	Implication for Design / AI-Assisted Conceptual Engineering
1:4 vs 1:16 — negligible difference (<5%)	Within the DNV-compliant zone, peak strain changes by less than 5% at all three stinger radii. The DNV 1:4 minimum is not an overbend strain optimum. Specifying a longer taper within code compliance adds component footprint with no strain benefit. Design recommendation: use 1:4 unless fabrication or fitment constraints require otherwise.
1:64 — step-change increase (+39% to +126%)	The 1:64 taper (footprint ~16D) exceeds the DNV 2% strain limit at R=70m (2.58%). The mechanism is geometric: the highly extended stiff zone adds to strain concentration at the neighboring pipe rather than relieving it. Recommended to avoid

International Journal for Research in Applied Science & Engineering Technology (IJRASET)
ISSN: 2321-9653; IC Value: 45.98; SJ Impact Factor: 7.538
Volume 14 Issue VII July 2026- Available at www.ijraset.com

Insight	Implication for Design / AI-Assisted Conceptual Engineering
Peak location: adjacent straight pipe	Peak strain is consistently at the pipeline element immediately outside the taper zone.
Stinger radius governs absolute strain level	Doubling the taper slope (1:4→1:16) within code saves <5% strain. Increasing R from 70→100m reduces strain by 43% (1.14%→0.65%). Stinger radius is the primary control parameter for taper transition strain management.

VIII. PARAMETRIC EVALUATION: TYPE A1 BEHAVIOUR – THICK SECTIONS

A. Study Detail

Studies in this section correspond to Series 3 in TABLE VI — pipelay with thick piping components. Three parametric sub-studies isolate the individual effects of wall thickness (Study 1), component length (Study 2), and inter-component spacing with two adjacent components (Study 3). Tapered transitions are not modelled; the aim is to characterize component geometry effects relative to each other, not to determine absolute installation strains. Standard mesh is used throughout (element length = max 2×OD); results are consistent within this series. See TABLE XVII and TABLE XVIII.TABLE XIII

TABLE XVII. BASIC MODEL PARAMETERS

Parameter	Value
Pipeline	406.4 mm OD (16 in) × 21 mm WT
Thick section wall thickness and Length	Varies. Refer below
Stinger configurations and Pipeline Tension	Varies. Refer below
Mesh detail	Standard mesh is used throughout (element length = max 2×OD); sufficient for this study – aim is to study results relative to parameter variation

TABLE XVIII. OVERVIEW — THREE PARAMETRIC SUB-STUDIES

#	Study Focus	Fixed Parameters	Varied Parameter	Cases	Stinger R
1	Wall Thickness Variation	Length=1000mm, T=100MT	WT: 1.5×, 2.0×, 2.5×	A1,A2,A3	70,85,100m
2	Length Variation	T=100MT WT=3.1×(R70), 2.5×(R85)	L: 2.5D,10D,20D(R70) 10D,20D,40D(R85)	B1,B2,B3,B4	70m & 85m
3	Two Components—Spacing Variation	WT=3.1×(65mm), T=100MT	Spacing	C1,C2,C3	70m only

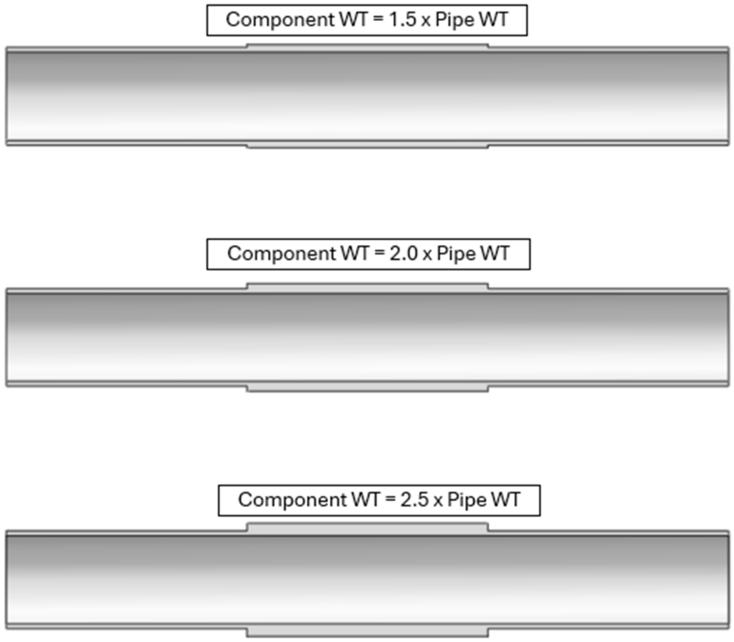

Fig. 35. Study 1: Thickness Variation

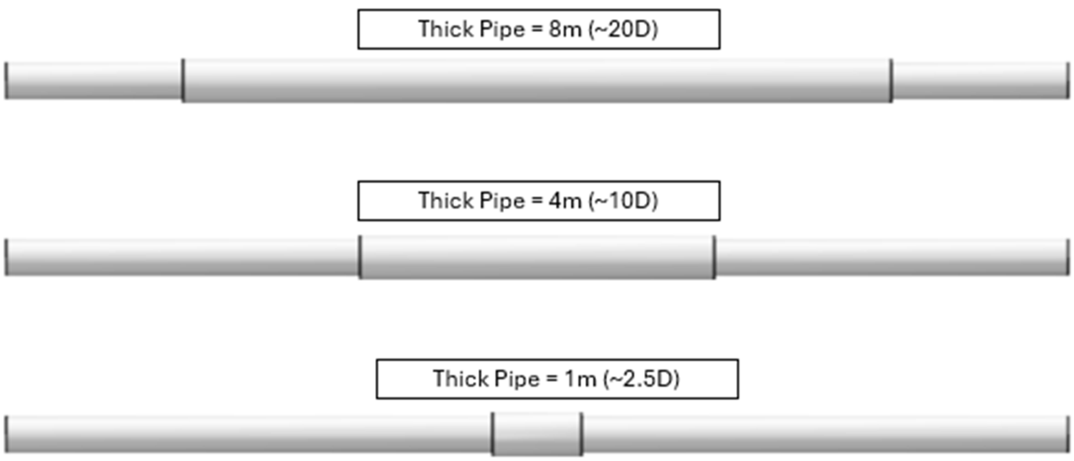

Fig. 36. Study 2: Thick Pipe Length Variation

B. Study 1 — Wall Thickness Variation: Input Cases

TABLE XIX. STUDY 1 INPUT CASES — WALL THICKNESS VARIATION (16IN PIPELINE, LENGTH FIXED)

Case	WT (mm)	WT Ratio	OD (mm)	Length	Tension	Stinger Radii
A1	32 mm	1.5×	406.4 mm	1000 mm (~2.5D)	100 MT	70m, 85m, 100m
A2	42 mm	2.0×	406.4 mm	1000 mm (~2.5D)	100 MT	70m, 85m, 100m
A3	53 mm	2.5×	406.4 mm	1000 mm (~2.5D)	100 MT	70m, 85m, 100m

C. Study 1 — Results: Peak Strain and Bending Moment

All cases exhibit Phase 1 behaviour (peak strain at 2nd stinger roller). Peak strain occurs at the pipe-to-component junction. Peak bending moment occurs near component midspan at the instant a roller is below midspan. TABLE XX presents strain results; TABLE XXI presents bending moments. Fig. 37 shows the strain trend for all three radii.

TABLE XX. Study 1 Results — Peak Pipeline Strain vs Wall Thickness Ratio

Case	WT (mm / ratio)	Peak Strain R=70m	Peak Strain R=85m	Peak Strain R=100m
A1	32mm / 1.5×	0.562%	0.473%	0.339%
A2	42mm / 2.0×	0.647%	0.508%	0.358%
A3	53mm / 2.5×	0.727%	0.556%	0.425%

Note 1: Location: Pipe-to-Component Junction (Phase 1, 2nd Stinger Roller).
Note 2: Pipeline plain pipe reference: 0.46% (R=70m), 0.38% (R=85m), 0.32% (R=100m) from §VI.

TABLE XXI. Study 1 Results — Peak Bending Moment vs Wall Thickness Ratio

Case	WT (mm / ratio)	Max BM R=70m	Max BM R=85m	Max BM R=100m
A1	32mm / 1.5×	1311 kN·m	1251 kN·m	1131 kN·m
A2	42mm / 2.0×	1347 kN·m	1288 kN·m	1144 kN·m
A3	53mm / 2.5×	1366 kN·m	1311 kN·m	1150 kN·m

Note 1: Location: Near component midspan, at instant roller is below midspan.

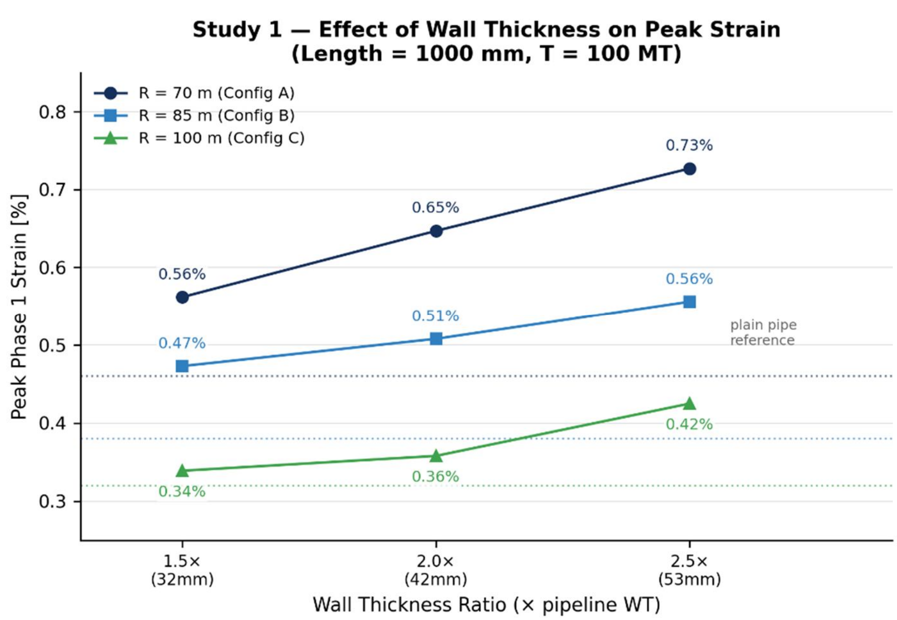

Fig. 37. Peak strain increases nearly linearly with WT ratio. Dashed lines show plain pipe reference at each R. Component increases strain by 22–33% above plain pipe baseline, with diminishing additional gain per unit thickness increase.

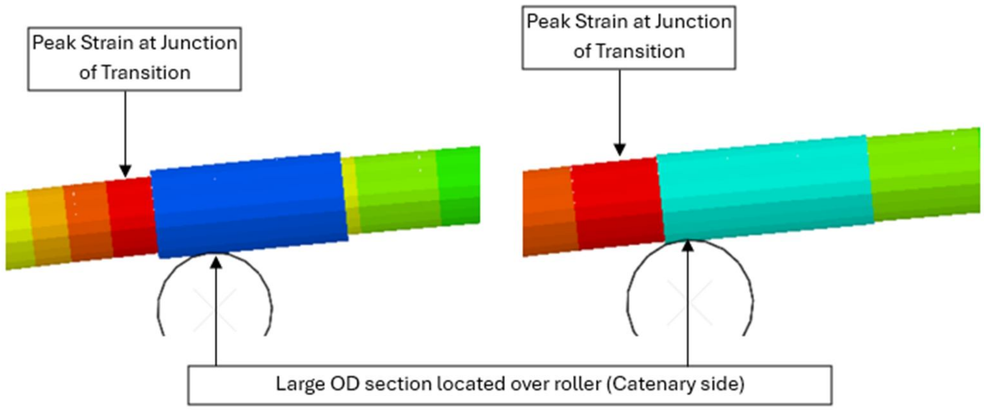

Fig. 38. Typical Peak Strain Characteristics – Wall thickness variation: 1.5 WT vs 2.5 WT (R = 70m)

D. Study 2 — Length Variation: Input Cases

TABLE XXII. Study 2 Input Cases — Length Variation (16in Pipeline)

Case	Length (mm)	L/D	WT at R=70m	WT at R=85m	Tension	Radii
B1 (R70)	1000 mm	~2.5D	65mm/3.1×	—	100 MT	R=70m only
B2 (R70+85)	4000 mm	~10D	65mm/3.1×	53mm/2.5×	100 MT	Both
B3 (R70+85)	8000 mm	~20D	65mm/3.1×	53mm/2.5×	100 MT	Both
B4 (R85)	16000 mm	~40D	—	53mm/2.5×	100 MT	R=85m only

E. Study 2 — Results: Peak Strain and Bending Moment

Length is the dominant driver of peak strain for thick pipe components. TABLE XXIII and TABLE XXIII present strain and BM results respectively. A critical behaviour change occurs at R=85m Case C (40D length): the peak strain does not increase significantly once the component is long enough to span multiple rollers . Fig. 42 shows the strain trend; Fig. 43 shows the bending moment trend. Fig. 39 shows the actual strain plot only model.

TABLE XXIII. Study 2 Results — Peak Pipeline Strain vs Component Length

Stinger R	Case / Length	Peak Strain	Location
R=70m	B1 (L=2.5D)	0.780%	Peak strain observed at Pipe/Component Jn.
R=70m	B2 (L=10D)	1.499%	
R=70m	B3 (L=20D)	2.514%	
R=85m	B2 (L=10D)	1.104%	Peak strain observed when component in Phase 1 (SR2)
R=85m	B3 (L=20D)	1.861%	
R=85m	B4 (L=40D)	1.914%	

International Journal for Research in Applied Science & Engineering Technology (IJRASET)
ISSN: 2321-9653; IC Value: 45.98; SJ Impact Factor: 7.538
Volume 14 Issue VII July 2026- Available at www.ijraset.com

TABLE XXIV. STUDY 2 RESULTS — PEAK BENDING MOMENT VS COMPONENT LENGTH

Stinger R	Case / Length	Peak BM (KN·m)	Location
R=70m	B1 (2.5D)	1384 KN·m	Component midspan / roller below midspan
R=70m	B2 (10D)	1650 KN·m	
R=70m	B3 (20D)	2223 KN·m	
R=85m	B2 (10D)	1581 KN·m	
R=85m	B3 (20D)	1977 KN·m	
R=85m	B4 (40D)	2883 KN·m	

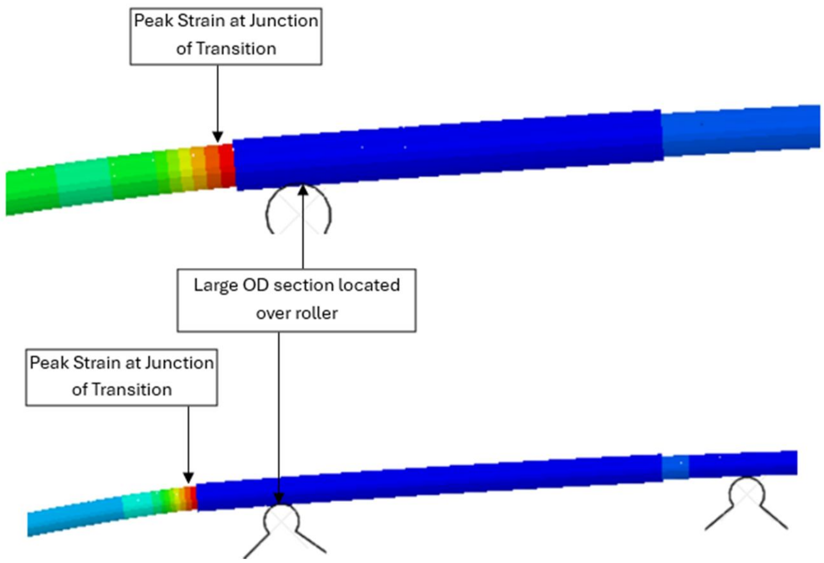

Fig. 39. Typical Peak Strain Characteristics – Length: 10D vs 20D (R = 70m)

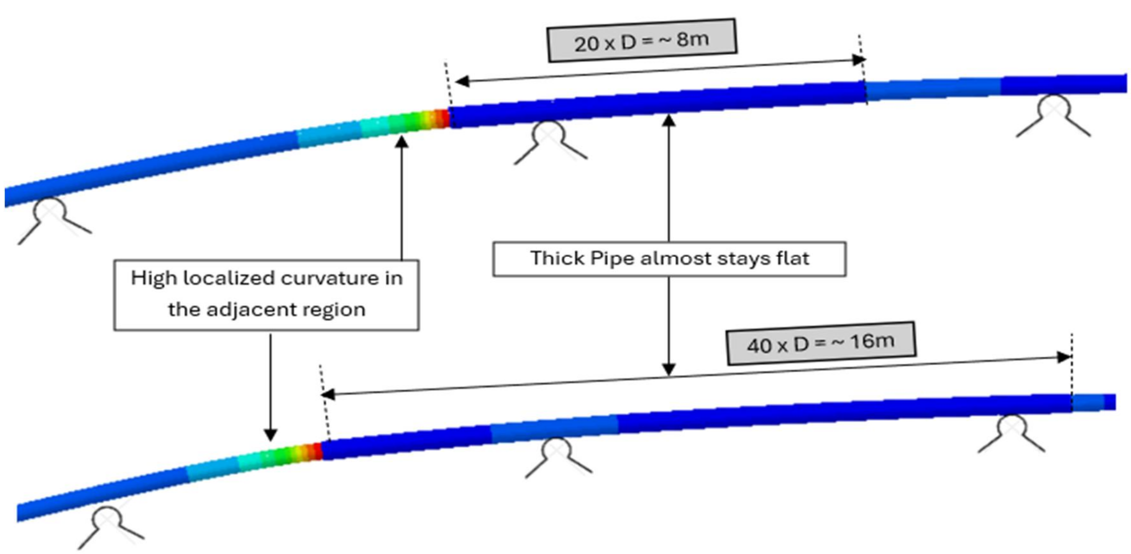

Fig. 40. Typical Curvature Distribution Behaviour – Length: 20D vs 40D (R = 85m)

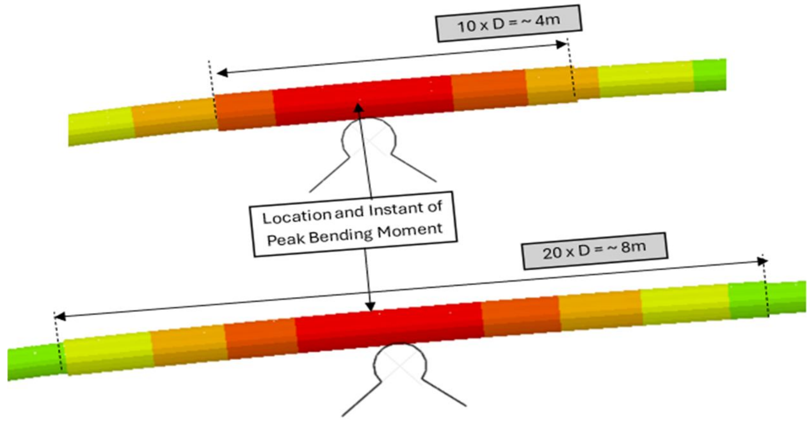

Fig. 41. Typical Bending Moment Distribution Behaviour – Length: 10D vs 20D (R = 85m)

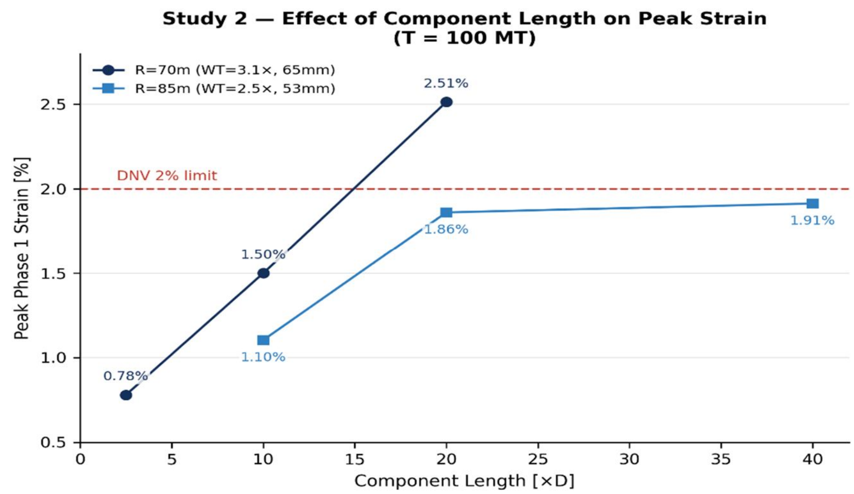

Fig. 42. Strain increases strongly with length. At R=70m the 20D case (2.514%) exceeds the DNV 2% limit. At R=85m the strain flattens from 20D to 40D (1.861%→1.914%) as the governing mechanism transitions.

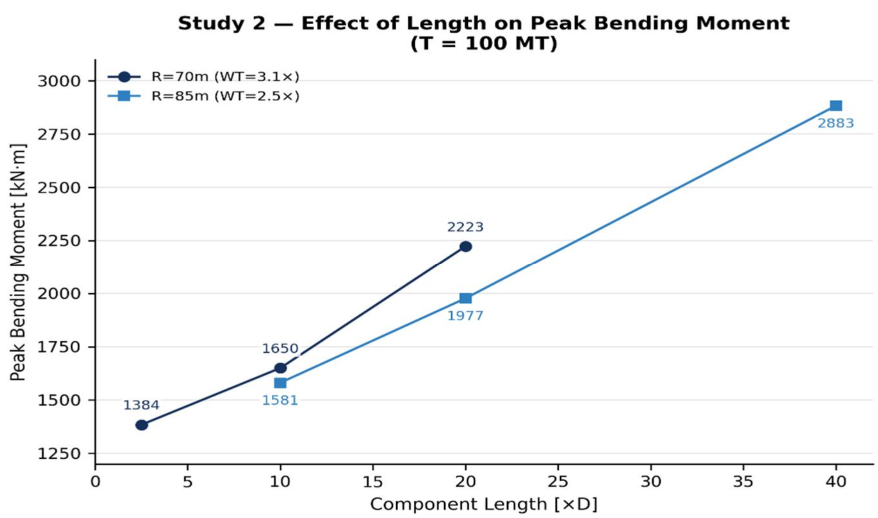

Fig. 43. Bending moment increases with length and shows no flattening at 40D, rising to 2883 kN·m.

ISSN: 2321-9653; IC Value: 45.98; SJ Impact Factor: 7.538
Volume 14 Issue VII July 2026- Available at www.ijraset.com

F. Study 3 — Spacing Variation (Two Components): Input Cases

TABLE XXV. STUDY 3 INPUT CASES — SPACING VARIATION: TWO IDENTICAL COMPONENTS (R=70M)

Case	Length (mm)	L/D	Clear Space (mm)	Sp/D	WT (mm/ratio)	Stinger R / Tension
C1	1000 mm	~2.5D	1000 mm	~2.5D	65mm / 3.1×	R=70m / T=100MT
C2	4000 mm	~10D	2000 mm	~5D	65mm / 3.1×	R=70m / T=100MT
C3	8000 mm	~20D	4000 mm	~10D	65mm / 3.1×	R=70m / T=100MT

G. Study 3 — Results

The study finds that strains reduce slightly with spacing, but the amount is negligible. See TABLE XXVI presents results.

TABLE XXVI. STUDY 3 RESULTS — TWO-COMPONENT VS SINGLE-COMPONENT STRAIN COMPARISON (R=70M, T=100MT)

Case	L per Piece	Spacing between Components	Two-Comp. Strain	BM
C1	1000mm (2.5D)	1000mm (2.5D)	0.771%	1384 kN·m
C2		4000mm (10D)	0.760%	1371 kN·m
C3		8000mm (20D)	0.751%	1365 kN·m

.

H. Design Insights — Cross-Study Summary

TABLE XXVII. DESIGN INSIGHTS — TYPE A1 THICK PIPE PARAMETRIC STUDIES

Insight	Implication for Design / AI-Assisted Conceptual Engineering
Wall thickness — moderate effect when the length is minor (Study 1)	• Increasing WT from 1.5× to 2.5× raises peak strain by ~29–25% above the 1.5× case at each radius. Effect is nearly linear. • Stinger radius remains the primary control: increasing R from 70⟶100m at fixed WT=2.5× reduces strain from 0.727% to 0.425% (−41%).
Length — dominant effect; critical beyond ~10D (Study 2)	• Strain increases strongly with length. At R=70m and Re=85m, the 20D component could cause pipeline strains exceeding DNV limit. • With mesh refinement during actual studies and Tapered transition inclusion, strains are expected to be larger. • Bending moments of long components are significantly higher than pipeline. Load capacity of the components could be exceeded and this means components require even higher wall thickness.
Two components	• Negligible strain reduction with increase in spacing between components
BM vs Strain diverge for Very Long Components (Study 2+3)	• For long components (~40D), bending moment continues to increase (2883 kN·m at R=85m, 40D) even as the peak strain plateau occurs.

©IJRASET: All Rights are Reserved

International Journal for Research in Applied Science & Engineering Technology (IJRASET)
ISSN: 2321-9653; IC Value: 45.98; SJ Impact Factor: 7.538
Volume 14 Issue VII July 2026- Available at www.ijraset.com

IX. PARAMETRIC EVALUATION: TYPE B1 BEHAVIOUR – OFFSET (SHROUD) ELEMENTS

A. Study Detail and Configuration

Studies in this section correspond to Series 4 in TABLE VI— pipelay with EA-O offset (shroud) elements producing Mechanical Behaviour Type B1. The shroud elevates the pipeline locally above the natural catenary, concentrating curvature at the catenary-side edge of the elevated zone.

TABLE XXVIII. BASIC PARAMETERS

Parameter	Value
Pipeline	406.4 mm OD (16 in) × 21 mm WT
Offset Geometry Parameters (L1, L2 and D)	Varies. Refer below.
Stinger configurations and Pipeline Tension	Varies. Refer below
Mesh detail	Standard mesh is used throughout (element length = max 2×OD); sufficient for this study – aim is to study results relative to parameter variation

Three geometric parameters are studied (see Fig. 44): the deep section length L1, the taper slope length L2, and the offset depth V (depth of deep section below pipe centerline).
Strain is reported across five pipeline regions defined in Fig. 45.

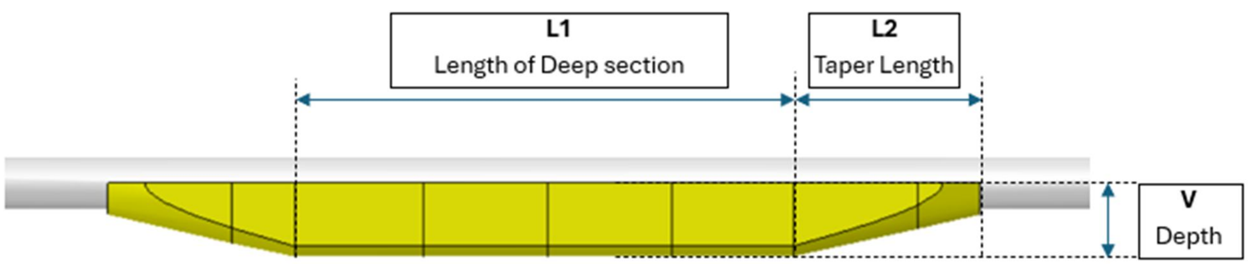

Fig. 44. Shroud Geometry Parameters Considered

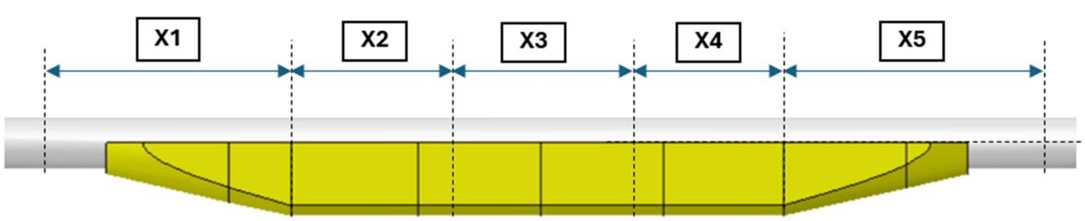

Fig. 45. Pipeline regions considered for Strain reporting

TABLE XXIX. PIPELINE REGION CLASSIFICATION — OFFSET (SHROUD) STUDIES

Region	**Location on Pipeline**	**Description**
X1	Upstream taper + outside shroud	Pipe over upstream taper and outside shroud — governed by plain-pipe catenary
X2	**Deep section — Catenary side 1/3**	Peak strain location in all cases. Governs design.

International Journal for Research in Applied Science & Engineering Technology (IJRASET)
ISSN: 2321-9653; IC Value: 45.98; SJ Impact Factor: 7.538
Volume 14 Issue VII July 2026- Available at www.ijraset.com

Region	Location on Pipeline	Description
X3	Deep section — Midspan	Intermediate strain; typically 65–75% of X2
X4	Deep section — Vessel side	Lowest strain; shows plateauing behaviour beyond V≈1.5D
X5	Downstream taper + outside shroud	Governed by plain-pipe catenary — not separately tabulated

Three stinger configurations are studied covering two stinger radii and two tension values. TABLE XXX provides the complete run matrix. Results are grouped into four parametric analyses.

TABLE XXX. COMPLETE RUN MATRIX — ALL 22 CASES, SORTED BY DEPTH V

Run	R	T	L1	L2	V	X2 Strain	Phase	Primary Study
S3-2	85m	100MT	10D	2.5D	**0.75D**	**0.62%**	Ph2	§IX.B,E
S3-3	85m	100MT	10D	2.5D	**1.0D**	**0.70%**	Ph2	§IX.B,E
S1-1	70m	120MT	5D	2.5D	**1.0D**	**0.81%**	Ph2	§IX.B
S1-2	70m	120MT	6D	2D	**1.0D**	**0.83%**	Ph2	§IX.B
S2-1	70m	100MT	2.5D	2D	**1.0D**	**0.78%**	Ph2	§IX.B,C
S2-2	70m	100MT	4D	5D	**1.0D**	**0.75%**	Ph2	§IX.C
S2-3	70m	100MT	10D	5D	**1.0D**	**0.76%**	Ph2	§IX.B,C
S2-4	70m	100MT	10D	1D	**1.0D**	**0.79%**	Ph2	§IX.D
S3-4	85m	100MT	10D	2.5D	**1.5D**	**0.95%**	Ph2	§IX.B,E
S1-3	70m	120MT	5D	2.5D	**1.5D**	**0.97%**	Ph2	§IX.B
S1-4	70m	120MT	6D	2D	**1.5D**	**1.05%**	Ph2	§IX.B
S2-5	70m	100MT	10D	5D	**1.5D**	**1.03%**	Ph2	§IX.B
S1-6	70m	120MT	2.5D	2D	**1.0D**	**0.83%**	Ph2	§IX.B
S1-7	70m	120MT	2.5D	2D	**1.5D**	**1.17%**	Ph2	§IX.B
S3-5	85m	100MT	10D	2.5D	**2.0D**	**1.20%**	Ph2	§IX.B,E
S1-5	70m	120MT	5D	2.5D	**2.0D**	**1.15%**	Ph2	§IX.B
S2-6	70m	100MT	10D	5D	**2.0D**	**1.23%**	Ph2	§IX.B,C
S2-7	70m	100MT	**25D**	2D	**2.0D**	**0.66/0.55%†**	Ph2	§IX.C
S2-8	70m	100MT	**50D**	2D	**2.0D**	**0.59%‡**	Ph2	§IX.C
S3-6	85m	100MT	10D	2.5D	**2.5D**	**1.51%**	Ph2	§IX.B,E
S3-7	85m	100MT	10D	2.5D	**3.0D**	**1.80%**	Ph2	§IX.B,E

† S2-7: single-roller contact gives 0.66%; double-roller contact gives 0.55%.
‡ S2-8: always minimum 2 rollers in contact (0.59%). Green shading = beneficial long-shroud effect.

International Journal for Research in Applied Science & Engineering Technology (IJRASET)
ISSN: 2321-9653; IC Value: 45.98; SJ Impact Factor: 7.538
Volume 14 Issue VII July 2026- Available at www.ijraset.com

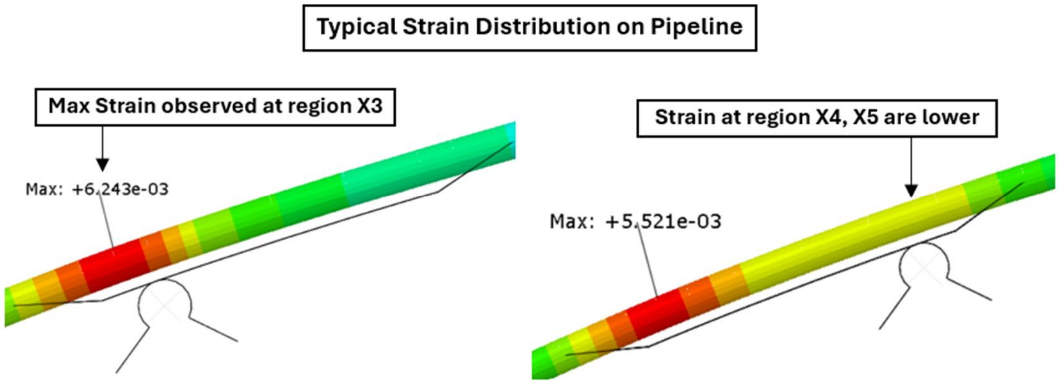

Fig. 46. Strain Distribution on Pipeline

B. Effect of Offset Depth V — Primary Governing Parameter

Offset depth V is the dominant parameter for shroud-type components. TABLE XXXI extracts the V-effect cases across all configurations and Fig. 47 presents the cross-study comparison. A near-linear relationship between V and peak strain at X2 is observed consistently across both stinger radii and both tension levels. At R=85m, V=3D produces X2=1.80%, approaching the DNV 2% limit.

TABLE XXXI. EFFECT OF OFFSET DEPTH V ON PEAK STRAIN AT X2 (ALL CONFIGURATIONS)

Configuration	V	L1	L2	X2 Strain	Phase	Note
R=70m, T=120MT	1.0D	5D	2.5D	0.808%	*Ph2*	
	1.5D	5D	2.5D	0.970%	*Ph2*	
	2.0D	5D	2.5D	1.15%	*Ph2*	
R=70m, T=100MT	1.0D	10D	5D	0.76%	*Ph2*	
	1.5D	10D	5D	1.03%	*Ph2*	
	2.0D	10D	5D	1.23%	*Ph2*	
R=85m, T=100MT	0.75D	10D	2.5D	0.62%	*Ph2*	*Shallowest tested*
	1.0D	10D	2.5D	0.70%	*Ph2*	
	1.5D	10D	2.5D	0.95%	*Ph2*	
	2.0D	10D	2.5D	1.20%	*Ph2*	
	2.5D	10D	2.5D	1.51%	*Ph2*	
	3.0D	10D	2.5D	1.80%	*Ph2*	*Deepest tested*

Three colour backgrounds denote three stinger configurations: amber=R70/T120, blue=R70/T100, green=R85/T100. Strain colour: green<1%, amber 1–1.5%, orange 1.5–2%, red≥2%.

International Journal for Research in Applied Science & Engineering Technology (IJRASET)
ISSN: 2321-9653; IC Value: 45.98; SJ Impact Factor: 7.538
Volume 14 Issue VII July 2026- Available at www.ijraset.com

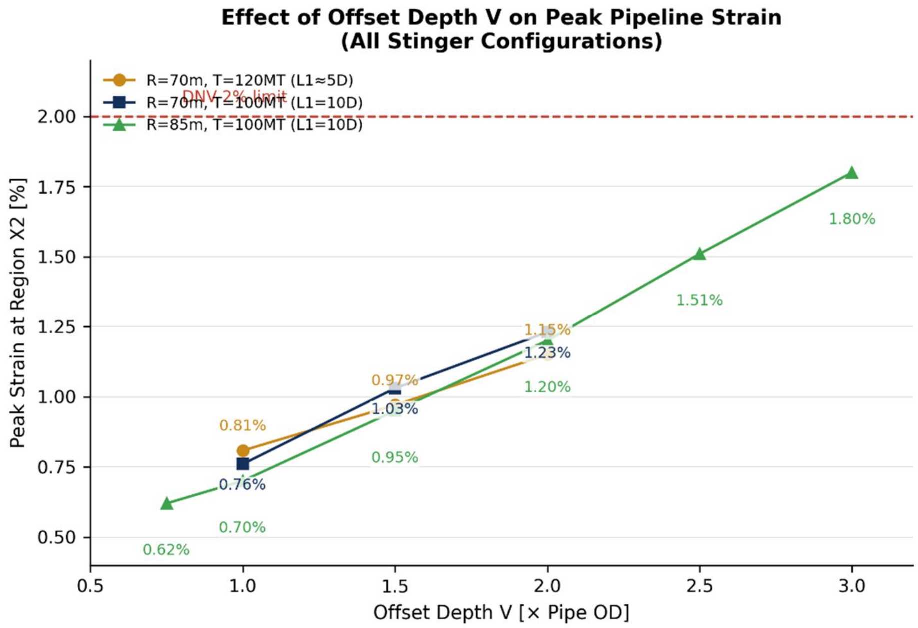

Fig. 47. Peak strain vs offset depth V across all three stinger configurations. Near-linear amplification is consistent regardless of R or T. Stinger radius shifts the curve vertically; increasing R from 70→100m reduces strain by ~10–20% at same V. Phase 1→2 transition occurs at V≈2D for R=70m.

C. *Effect of Deep Section Length L1*

TABLE XXXII isolates the effect of deep section length L1, with two distinct regimes. For moderate lengths (L1=2.5D to 10D) at V=1D, strain varies by less than 5% — L1 has negligible effect. For very long shrouds (L1≥25D) at V=2D, a dramatic strain reduction occurs as the shroud shifts from single-roller to double-roller contact during stinger passage.

TABLE XXXII. Effect of Deep Section Length L1 — Moderate Range (V=1D) and Long-Shroud Regime (V=2D)

Case	L1	L2	V	X2 Strain	Phase	Observation
S2-1	2.5D	2D	1.0D	0.78%	*Ph2*	*V=1D baseline*
S2-2	4D	5D	1.0D	0.75%	*Ph2*	*L1 doubled — strain unchanged*
S2-3	10D	5D	1.0D	0.76%	*Ph2*	*L1 quadrupled — strain unchanged*
S2-6	10D	5D	2.0D	1.23%	*Ph2*	*V=2D baseline (single-roller)*
S2-7	25D	2D	2.0D	0.66% / 0.55%†	*Ph2*	*⚠Long shroud: single→dual roller transition*
S2-8	50D	2D	2.0D	0.59%‡	*Ph2*	*⚠Very long: always dual-roller contact*

† S2-7: 0.66% during single-roller contact; 0.55% during double-roller contact passage.
‡ S2-8 (L1=50D): shroud always spans two roller spacings; always minimum 2-roller contact (0.59%).
This long-shroud produces a structural zone spanning multiple rollers that reduces peak curvature at the end junction.

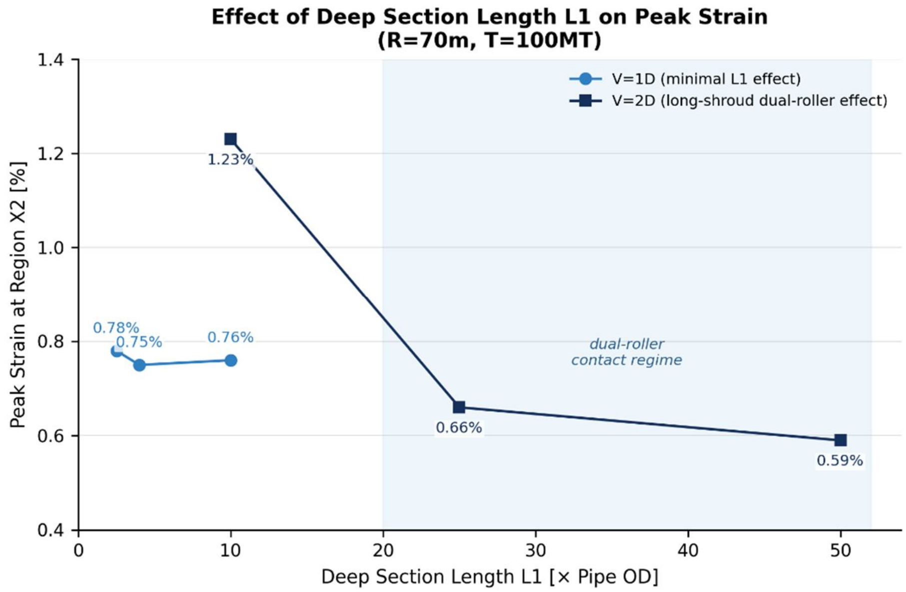

Fig. 48. Effect of L1 on peak strain. At V=1D (blue): strain is flat across 2.5–10D — L1 has negligible effect. At V=2D (navy): dramatic reduction at L1=25D and 50D as the long-shroud dual-roller mechanism engages. Same mechanism as §VIII Study 3.

D. Effect of Taper Slope Length L2

TABLE XXXIII compares two cases with identical L1 and V but different taper slope lengths L2. The difference is less than 4% — L2 has minimal effect on peak strain within the range studied and does not require optimization for strain reduction.

TABLE XXXIII. EFFECT OF TAPER SLOPE LENGTH L2 (L1=10D, V=1D, R=70M, T=100MT)

Case	L1	L2	V	X2 Strain	Phase	Observation
S2-3	10D	**5D**	1.0D	**0.76%**	*Ph2*	*Long taper reference*
S2-4	10D	**1D**	1.0D	**0.79%**	*Ph2*	*+0.03 pp with short taper — within modelling noise*

L2 varies from 1D (steep taper) to 5D (shallow taper). The 0.03 pp difference is within modelling uncertainty. No optimization of L2 for strain reduction is warranted.

E. Multi-Region Strain Distribution (X2, X3, X4)

Study S3 (R=85m, L1=10D, L2=2.5D) provides the most complete dataset for strain distribution across the deep section. TABLE XXXIV and Fig. 49 show strain at regions X2, X3, and X4 as V increases from 0.75D to 3.0D. Key observations: X2 (catenary side) consistently governs; X3 (midspan) is approximately 65–70% of X2; X4 (vessel side) plateaus beyond V≈1.5D while X2 and X3 continue to rise.

TABLE XXXIV. MULTI-REGION STRAIN DISTRIBUTION VS OFFSET DEPTH V (R=85M, T=100MT, L1=10D, L2=2.5D)

V (depth)	X2 — Catenary (Peak)	X3 — Midspan	X4 — Vessel	X3/X2 Ratio	Phase
0.75D	0.62%	0.42%	0.35%	68%	*Ph2*
1.0D	0.70%	0.55%	0.43%	79%	*Ph2*
1.5D	0.95%	0.75%	*0.58% ✓*	79%	*Ph2*

ISSN: 2321-9653; IC Value: 45.98; SJ Impact Factor: 7.538
Volume 14 Issue VII July 2026- Available at www.ijraset.com

V (depth)	X2 — Catenary (Peak)	X3 — Midspan	X4 — Vessel	X3/X2 Ratio	Phase
2.0D	1.20%	0.88%	*0.58% ✓*	73%	*Ph2*
2.5D	1.51%	1.07%	0.62%	71%	*Ph2*
3.0D	1.80%	1.20%	0.67%	67%	*Ph2*

✓ indicates X4 plateau (0.58–0.67%) — vessel-side strain does not amplify proportionally beyond V≈1.5D.

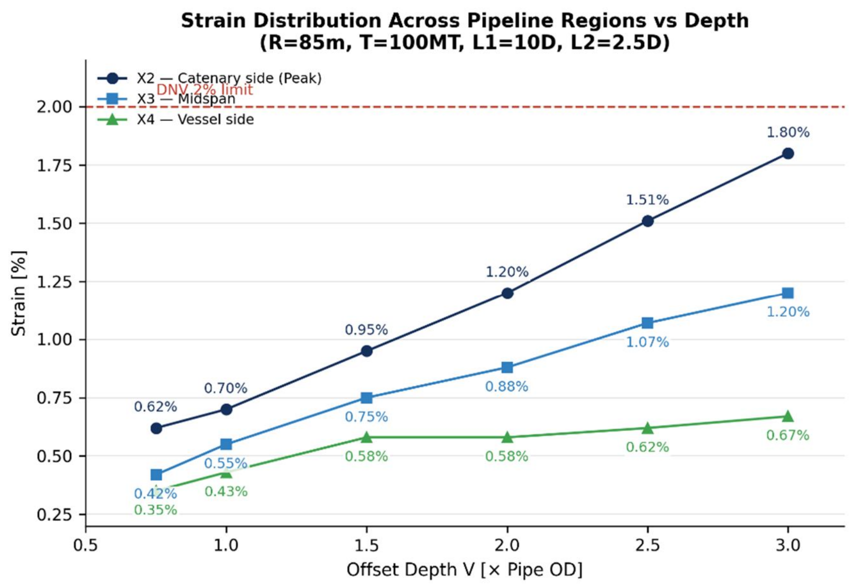

Fig. 49. Strain at regions X2, X3, X4 vs offset depth V. X2 (peak) is nearly linear; X4 plateaus beyond V≈1.5D. The catenary-side end of the deep section is the critical fatigue location for all depths tested.

F. Design Insights

TABLE XXXV. DESIGN INSIGHTS — TYPE B1 OFFSET (SHROUD) ELEMENTS

Insight	Implication for Design / AI-Assisted Conceptual Engineering
V dominates — target V≤1.0D where possible	Strain at X2 increases nearly linearly with V regardless of R or T. At R=85m: V=1D→0.70%, V=2D→1.20%, V=3D→1.80%. Each 1D increase in depth adds ~0.35–0.55% strain. Minimising offset depth is the single most effective design action for shroud elements.
L1 is insensitive in normal range (2.5D–10D)	Strain changes by <5% as L1 varies from 2.5D to 10D at V=1D. Component length can be selected for operational or structural reasons without strain penalty within this range.
Long shrouds (≥25D): dual-roller regime reduces strain	At V=2D: L1=10D gives 1.23%; L1=25D gives 0.55–0.66%; L1=50D gives 0.59%. Very long shrouds force dual-roller contact and reduce peak strain by ~50–55%. This is the same mechanism as the two-component sequence effect in §VIII Study 3. Long shrouds carry cost/complexity penalties but may be viable where high V is unavoidable.
L2 (taper length) — negligible effect	Varying L2 from 1D to 5D changes strain by <4%..

Insight	Implication for Design / AI-Assisted Conceptual Engineering
Governing phase: Phase 2 in most cases	Unlike thick pipe components (§VIII, Phase 1 dominant), shroud elements govern in Phase 2 (elastic mid-roller bending). Phase 1 is only observed for shallow shrouds (V≤1.5D) at large L1 and higher tension. The shroud modifies the global curvature profile of the stinger, shifting the critical event from the first-roller plastic bending to the mid-stinger elastic cycle.
Strain gradient: X2>>X3>X4; X4 plateaus	At V=2D: X2=1.20%, X3=0.88%, X4=0.58%. X4 plateaus beyond V≈1.5D while X2 and X3 continue rising. The catenary-side end of the deep section is the fatigue-critical S-Lay location. Fatigue assessment should focus on the X2 region.

X. PARAMETRIC EVALUATION: TYPE C1 BEHAVIOUR – OFFSET ELEMENTS + THICK PIPE

A. Study Detail and Configuration

This study correspond to Series 5 in TABLE VI — pipelay with a combination of EA-O offset (shroud) elements and thick pipe (IW-P/IW-A) components, producing Mechanical Behaviour Type C1. Type C1 is the combined type: both stiffness discontinuity (Type A mechanism) and elevation offset (Type B1 mechanism) act simultaneously. The aim is to quantify how the combination compares with the isolated Type B1 (shroud-only) baseline from §IX, and to identify which parameters of the thick pipe geometry and location most influence the combined response.

The shroud geometry is held fixed throughout (L1=10D, L2=2.5D, V=1D, R=85m, T=100MT), matching the §IX reference case (S3-3) which produced X2=0.70% for the shroud alone. Two series of studies vary the thick pipe geometry (Series 1) and location (Series 2) within the shroud deep section.

TABLE XXXVI. FIXED STUDY PARAMETERS — TYPE C1 SERIES

Parameter	Value
Pipeline	406.4 mm OD (16 in) × 21 mm WT
Shroud geometry (fixed)	L1 = 10D, L2 = 2.5D, V = 1D (see Fig. 44)
Stinger configuration	R = 85 m, T = 100 MT
Mesh	Standard mesh — element length = max 2×OD (aim: relative comparison, not absolute strains)
Shroud-only baseline (from §IX, S3-3)	X2 = 0.70%, Phase 2 (reference for all comparisons)
Thick pipe geometry and location	Varies: see Series 1 and Series 2 below

TABLE XXXVII. STUDY PLAN — TWO SERIES (5 CASES TOTAL)

Series	Variable (Thick Pipe)	Cases	Objective
1	Thick pipe length (5D vs 10D)	Case 1: 5D, centered in X3 (extends into X2 & X4) Case 2: 10D, spans X2, X3 and X4	Effect of thick pipe size within the shroud deep section
2	Thick pipe location (2.5D, at X2 vs X3 vs X4)	Case 1: 2.5D at X2 (catenary 1/3) Case 2: 2.5D at X3 (midspan) Case 3: 2.5D at X4 (vessel side)	Effect of thick pipe axial position within the deep section

B. Series 1 — Effect of Thick Pipe Size

Series 1 places a thick pipe inside the shroud deep section and varies its length. In Case 1 (5D length), the component is centered in region X3 and partially extends into X2 and X4. In Case 2 (10D length), the component spans all three deep section regions (X2, X3, X4). Both cases are compared against the shroud-only baseline (X2=0.70%).

TABLE XXXVIII. SERIES 1 INPUT CASES — THICK PIPE LENGTH VARIATION

Case	Thick Pipe Length	Location / Coverage	Shroud Geometry
1	5D	Centred in X3; partially extends into X2 and X4 (see Fig. 50)	*L1=10D, L2=2.5D, V=1D*
2	10D	Spans X2, X3, and X4 fully (see Fig. 51)	*L1=10D, L2=2.5D, V=1D*

Fig. 50 and Fig. 51 presents illustrations of Cases 1 and 2 of Series 1.

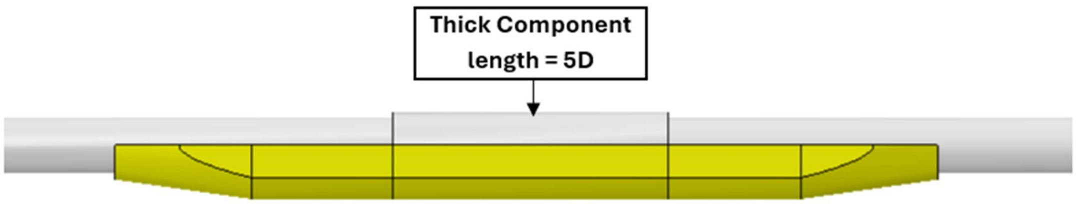

Fig. 50. Case 1 – Thick component of length 5D in combination with shroud

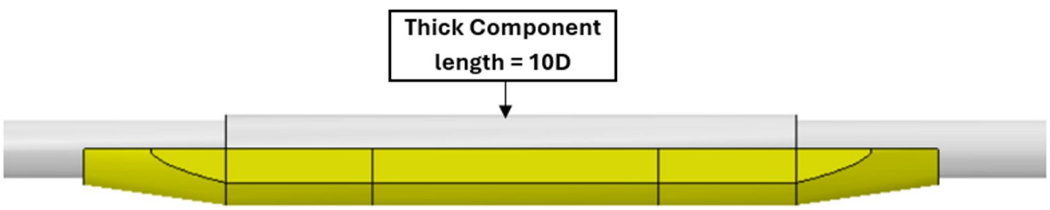

Fig. 51. Case 2 – Thick component of length 10D in combination with shroud

TABLE XXXIX. SERIES 1 RESULTS — EFFECT OF THICK PIPE LENGTH (R=85M, T=100MT)

Case	Thick Pipe Length	Max Strain X2 (Peak)	Max BM (Thick body)	Phase	Peak Location / Note
B1 ref	Shroud only	0.70%	—	Ph2	§IX baseline (S3-3, same config)
1	**5D**	**0.952%**	1405 kN·m	Ph2	Pipeline body at X2 | +36% above B1 baseline
2	**10D**	**1.26%**	1555 kN·m	Ph2	Pipe-to-component junction at X2 | +80% above baseline

Reference row (blue): shroud-only baseline from §IX (same stinger config, V=1D, L1=10D). All Type C1 results exceed this baseline. BM on thick component body increases with component length.

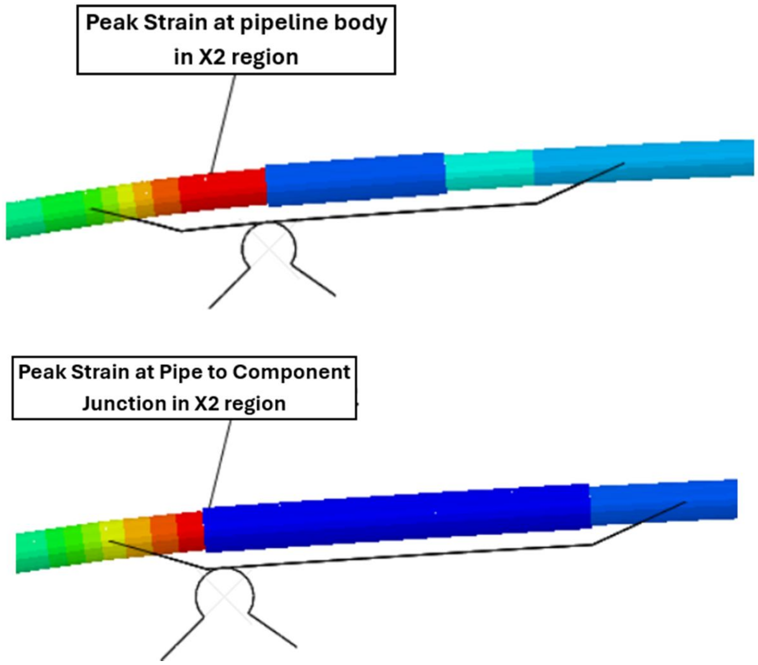

Fig. 52. Strain distribution for Series 1 – Cases 1 and 2

C. Series 2 — Effect of Thick Pipe Location

Series 2 holds thick pipe size fixed at 2.5D and varies its axial position within the shroud deep section: at X2 (catenary side), X3 (midspan), or X4 (vessel side). This isolates the effect of position from size. A key finding emerges: Cases 2 (X3) and 3 (X4) produce identical results, while Case 1 (X2) is significantly worse.

TABLE XL. SERIES 2 INPUT CASES — THICK PIPE LOCATION VARIATION (LENGTH = 2.5D FIXED)

Case	Thick Pipe Length	Location within Deep Section	Shroud Geometry
1	2.5D	X2 — Catenary side 1/3 of deep section (peak strain region)	*L1=10D, L2=2.5D, V=1D*
2	2.5D	X3 — Midspan of deep section	*L1=10D, L2=2.5D, V=1D*
3	2.5D	X4 — Vessel side 1/3 of deep section	*L1=10D, L2=2.5D, V=1D*

Fig. 53, Fig. 54 and Fig. 55 presents illustrations of Cases 1 to 3 of Series 2.

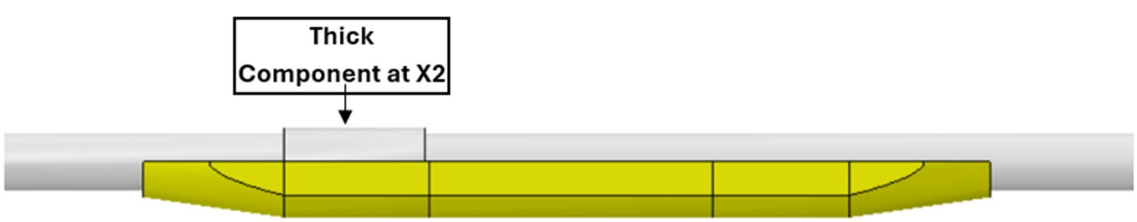

Fig. 53. Case 1 – Thick component of length 2.5D located in X2 region

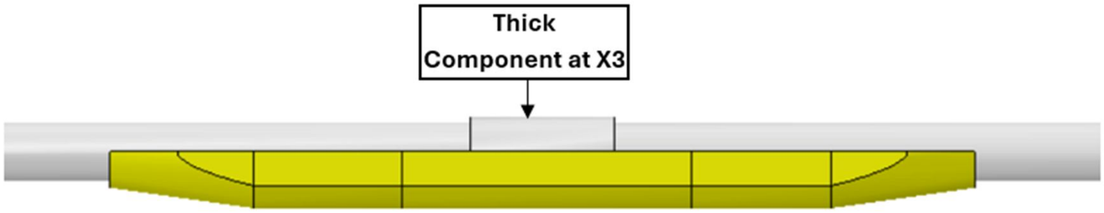

Fig. 54. Case 2 – Thick component of length 2.5D located in X3 region

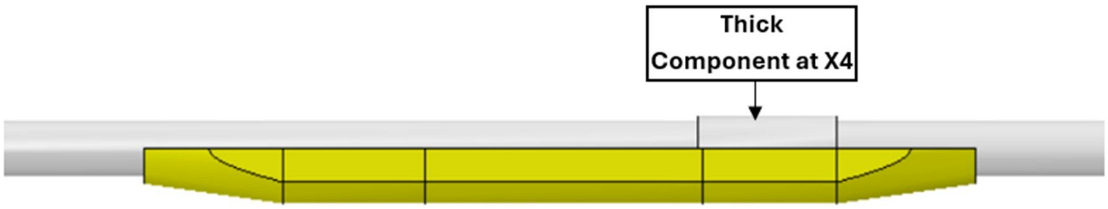

Fig. 55. Case 3 – Thick component of length 2.5D located in X4 region

TABLE XLI. SERIES 2 RESULTS — EFFECT OF THICK PIPE LOCATION (R=85M, T=100MT)

Case	Thick Pipe Location	Strain X2 (Peak)	Strain X4	Max BM (Thick body)	Phase	Peak Location
B1 ref	*Shroud only (no thick pipe)*	*0.70%*	*0.35%*	*—*	*Ph2*	*§IX baseline*
1	**X2 — Catenary 1/3**	**0.901%**	0.49%	1362 kN·m	*Ph2*	*Pipe/Component junction at X2*
2	X3 — Midspan	**0.744%**	0.59%	1310 kN·m	*Ph2*	*Pipeline body at X2*
3	X4 — Vessel side 1/3	**0.744%**	0.57%	1271 kN·m	*Ph2*	*Pipeline body at X2 (cf. Case 2)*

Cases 2 and 3 produce nearly identical results (0.737% vs 0.744% — within 1% of each other), confirming that X3 and X4 placement are mechanically very similar at V=1D. The small difference falls within typical modelling uncertainty. Peak strain is always at X2 regardless of thick pipe location.
Case 1 (thick pipe at X2) is highlighted orange: the thick pipe occupies the peak-strain region of the shroud, creating a stiffness discontinuity precisely where the catenary curvature is highest. This amplifies strain at the pipe-to-component junction.

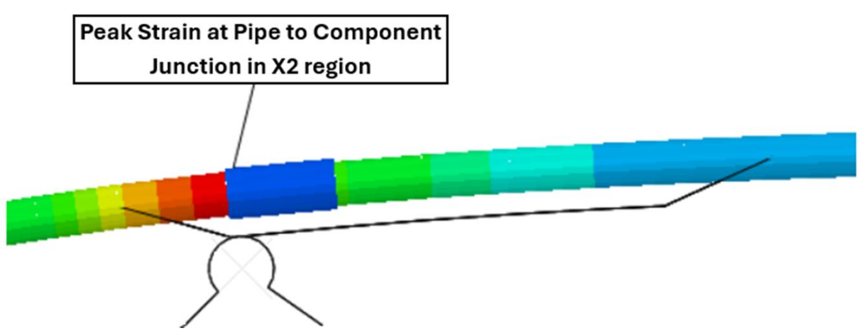

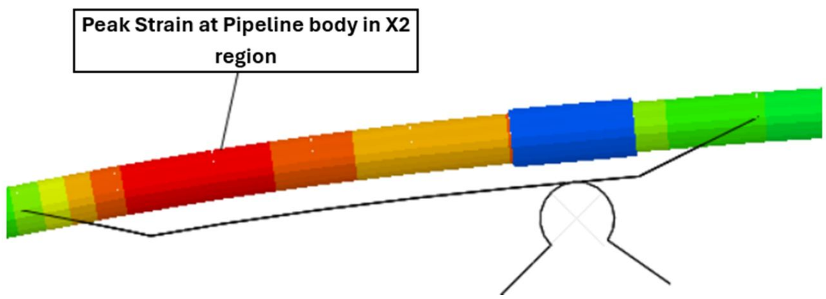

Fig. 56. Strain distribution for Series 2 – Cases 1 and 3

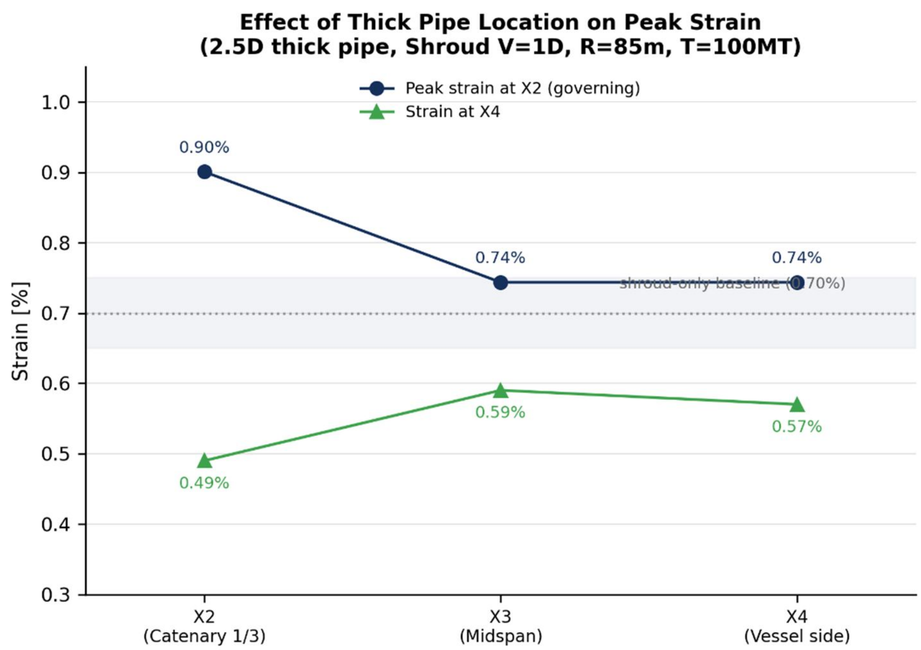

Fig. 57. Effect of thick pipe location on peak strain (Series 2). Placing the thick pipe at X2 (catenary side) is significantly worse than X3 or X4. Cases 2 and 3 (X3, X4) are identical, showing that the deep-section interior position does not matter for this shroud configuration.

D. Cross-Comparison — Type C1 vs Isolated Component Types

TABLE XLII presents all study results alongside the isolated component baselines from §VIII (thick pipe alone, approximate) and §IX (shroud alone). Fig. 58 provides the visual comparison. The combined Type C1 system always exceeds both isolated component responses. However, the degree of compounding depends critically on the thick pipe geometry and location.

TABLE XLII. CROSS-COMPARISON — TYPE A1, B1, AND C1 AT SAME STINGER CONFIGURATION (R=85M, T=100MT)

Configuration	Peak Strain	BM (Thick body)	Phase	Type	Reference
Thick pipe alone (2.5D, R=85m)	**~0.47%†**	—	*Ph2*	**A1**	*§VIII approx.*
Shroud alone (V=1D, L1=10D)	**0.70%**	—	*Ph2*	**B1**	*§IX S3-3*
C1: Thick at X3/X4 (2.5D, best	**0.737–0.744%**	1310 kN·m	*Ph2*	**C1**	*Ser.2 C2/C3*

Configuration	Peak Strain	BM (Thick body)	Phase	Type	Reference
location)					
C1: Thick at X2 (2.5D, worst location)	**0.901%**	1362 kN·m	*Ph2*	**C1**	*Ser.2 C1*
C1: Thick 5D (centred in X3)	**0.952%**	1405 kN·m	*Ph2*	**C1**	*Ser.1 C1*
C1: Thick 10D (spans X2–X4)	**1.26%**	1555 kN·m	*Ph2*	**C1**	*Ser.1 C2*

† Thick pipe alone at R=85m: approximate value from §VIII Study 1 Case A (2.5D, T=100MT). Exact WT of the §X thick pipe is not stated; value used for indicative comparison only.

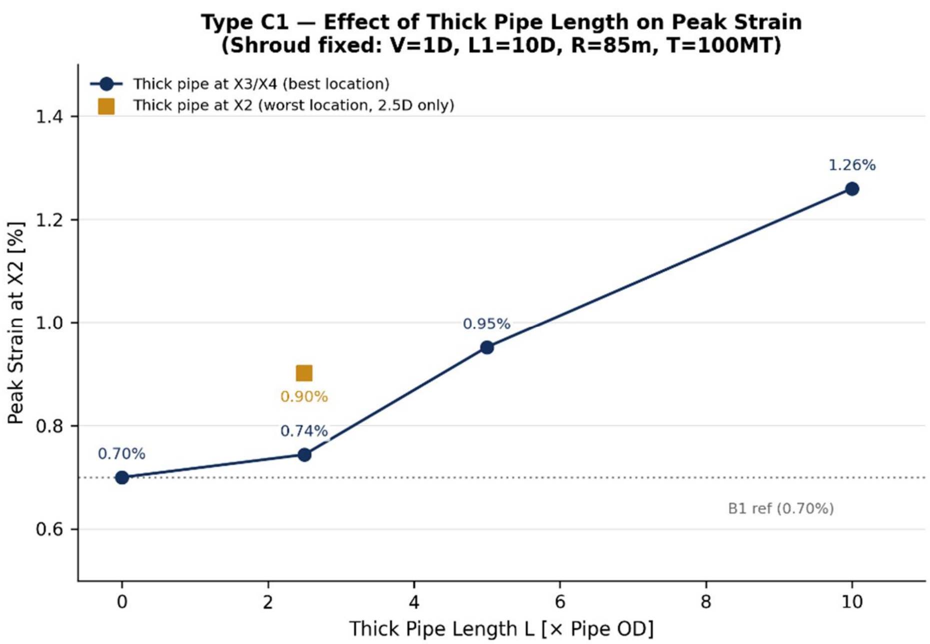

Fig. 58. Cross-comparison of Type A1 (thick pipe), B1 (shroud), and C1 (combined) peak strain. The combined configuration always exceeds both isolated types. Thick pipe at X3/X4 adds minimal strain above the shroud baseline (+5%); thick pipe at X2 or large size creates significant amplification.

E. Design Insights

TABLE XLIII. DESIGN INSIGHTS — TYPE C1 OFFSET + THICK PIPE COMBINED

Insight	Implication for Design / AI-Assisted Conceptual Engineering
Type C1 always exceeds isolated B1 or A1	The combined system (shroud + thick pipe) always produces higher peak strain than either component in isolation. Non-additive superposition applies: C1 strain is not simply A1 + B1. Type C1 systems require dedicated analysis; isolated-component strain estimates are unconservative.
Thick pipe location within the shroud is the critical variable	Placing the thick pipe at X2 (catenary side) gives 0.901% vs 0.737–0.744% for X3/X4 — a +18–22% penalty. X2 is already the peak-strain region of the shroud; adding a stiffness discontinuity there amplifies it further. Design rule: keep the thick pipe out of X2 (catenary 1/3 of the deep section) where possible.
X3 and X4 placement are equivalent	Cases 2 (X3) and 3 (X4) of Series 2 produce very similar results (0.737% and

Insight	Implication for Design / AI-Assisted Conceptual Engineering
at V=1D	0.744% respectively — within 1% of each other). This indicates that for shallow shrouds (V=1D), the interior of the deep section is mechanically uniform from the pipeline's curvature perspective. The distinction between X3 and X4 placement is not significant at this depth.
Thick pipe size matters: 2.5D→5D→10D amplifies strain substantially	Holding location constant (X3): 2.5D→0.737–0.744%, 5D→0.952%, 10D→1.26% (inferred from location pattern). The 10D case approaches the DNV 2% limit (1.26% at R=85m). Larger thick pipe sizes should be avoided in the catenary zone or combined with a larger stinger radius.
BM on thick component scales with size	BM ranges from 1310 kNm (2.5D) to 1555 kNm (10D). Structural capacity of the thick-wall component body must be checked independently using ASME VIII criteria. The combined loading environment (bending + internal pressure) governs the thick component design.
Governing phase remains Phase 2 for all cases	Type C1 governs in Phase 2 (mid-roller elastic bending), inherited from the Type B1 (shroud) contribution. The shroud's elevation effect dominates the phase selection; the thick pipe stiffness effect modifies the strain magnitude but does not change the governing phase.

XI. DISCUSSION

A. Cross-Cutting Findings

Position governs, not just magnitude. For every mechanical type studied, peak strain consistently locates at the catenary-side edge of the discontinuity — the pipe-to-component junction for Type A (§VIII), region X2 for Type B (§IX), and again X2 for Type C (§X). Placing a stiffness discontinuity inside this zone (Type C1, thick pipe at X2) produces the worst outcome tested, while identical geometry placed at X3 or X4 is materially better. This suggests that where a stiff or elevated feature sits relative to the catenary-side roller matters as much as what the feature is — a principle a future Step 3 (Intuitive Assembly) tool would need to encode explicitly.

Long components can relieve strain, not just amplify it. Two independent series — the two-component spacing study (§VIII.G) and the long-shroud study (§IX.C, L1 ≥ 25D) — show that once a structural zone becomes long enough to span more than one roller spacing, it forces simultaneous dual-roller contact, and peak strain drops rather than rises. This is counterintuitive relative to the otherwise-monotonic length effect seen at moderate lengths (§VIII.D, L ≤ 20D), and it means "longer is worse" is only a local rule, not a global one.

Strain and bending moment can diverge. For very long thick-pipe components, peak pipeline strain plateaus or falls (§VIII Studies 2–3) even as peak bending moment in the component body keeps rising (§VIII.D, 2883 kN·m at 40D). Because the pipeline is governed by DNV-ST-F101 displacement-controlled criteria while the component body is governed by ASME VIII load-controlled criteria (§II), a configuration that looks favourable on the DNV strain check can simultaneously be approaching its ASME capacity limit. Both checks must be carried independently — this is a direct consequence of the code split established in Section II.

Code minimums are not strain optima, and non-additivity limits simple superposition. The taper-slope study (§VII) shows the DNV 1:4 minimum sits in a flat, near-optimal region — tightening it buys negligible benefit, but relaxing it past ~1:16 produces a step-change strain penalty. Separately, the combined Type C1 results (§X.D) show peak strain always exceeds both isolated Type A and Type B baselines, and does so non-additively — C1 strain cannot be estimated by summing isolated A1 and B1 responses. Both findings caution against two tempting shortcuts: treating code-minimum geometry as strain-optimal, and treating assembly-level strain as a simple sum of component-level effects.

B. Limitations

The results should be read as relative trends, not absolute design values, for three reasons. First, the single-roller contact model adopted throughout (§IV.C) is known to overestimate peak strain by roughly 20% relative to a two-roller model (Yun et al.[19]);

this conservatism is consistent within each series but means absolute strain values should not be used directly for code compliance without a two-roller or full roller-box model. Second, mesh density differs between series — the taper study (§VII) uses a very fine mesh at the transition, while the thick-section, shroud, and combined studies (§VIII–X) use a standard mesh — so absolute magnitudes are not strictly comparable across series, though trends within each series remain valid. Third, the parametric matrix is built around a single 16-inch pipeline geometry; the diameter and tension sensitivity established in §VI (Study 2) supports generalization but has not been verified across the full range of pipe sizes an ILT programme would encounter.

XII. CONCLUSIONS

This paper introduced a dual-classification framework — a physical IW/EA taxonomy describing how inline hardware connects to the pipeline, and a mechanical Type A/B/C taxonomy describing the strain-amplification mechanism each connection produces — that bridges the hardware design domain (DNV-ST-F101, ASME VIII) and the S-Lay installation analysis domain. Through five progressive series of Abaqus parametric finite element analyses, it characterized the isolated and combined behaviour of Types A1, B1, and C1:

– Type A1 (stiffness-dominant): taper slope has negligible effect within the DNV-compliant range (1:4–1:16, <5% difference) but produces a step-change strain penalty beyond it; thick-section length is the dominant parameter and becomes critical beyond ~10D; inter-component spacing has negligible effect; very long components can enter a dual-roller relief regime.

– Type B1 (elevation-dominant): offset depth V is the dominant, near-linearly-acting parameter; deep-section length and taper slope are largely insensitive in the normal range; very long shrouds (≥25D) trigger the same dual-roller relief mechanism seen in Type A.

– Type C1 (combined): always exceeds both isolated Type A and Type B responses; the location of a stiffness discontinuity within an elevated zone is the critical design variable, with placement in the catenary-side peak-strain region producing an 18–22% penalty over placement elsewhere.

Together, these findings constitute the quantitative design intuition — Steps 1 and 2 of the seven-step AI-assisted conceptual engineering programme proposed in Section III — needed to support informed, code-aware conceptual design of subsea inline structural assemblies before detailed finite element analysis is undertaken

XIII. FUTURE WORK

First, completing the design intuition layer requires characterizing Types A2, B2, and C2 — the lumped-stiffness and concentrated-elevation behaviour exhibited by EA-SB, EA-ST, and EA-R structures, which this paper did not cover (Table IV).

Second, Steps 3 through 7 of the development programme — Intuitive Assembly, Simplified Analysis, Design Code Assessment, Iterative Analysis, and Configuration Optimization — build on this foundation to move from component-level intuition toward automated, code-checked assembly-level design.

REFERENCES

[1] Y. Bai and Q. Bai, Subsea Pipeline Design, Analysis and Installation. Oxford: Gulf Professional Publishing, 2014, ch. 33.
[2] A. Palmer and R. King, Subsea Pipeline Engineering, 2nd ed. Tulsa: PennWell, 2008.
[3] D. Perinet and I. Frazer, “Strain Criteria for Deep Water Pipe Laying Operations,” Offshore Technology Conference, OTC 19329, Houston, Texas, May 2008. DOI: 10.4043/19329-MS.
[4] R. O’Grady and A. Harte, “Localised assessment of pipeline integrity during ultra-deep S-lay installation,” Ocean Engineering, vol. 68, pp. 27–37, 2013.
[5] DNV-ST-F101, Submarine Pipeline Systems. Det Norske Veritas, October 2017.
[6] K. Huang, A. Ji, and E. Uribe, “Deepwater In-Line SLED Installation Methods and its Application to Frade Project,” Offshore Technology Conference, OTC 19805, Houston, Texas, May 2009.
[7] J. K. Antani, W. T. Dick, D. Balch, and T. van der Leij, “Design, Fabrication and Installation of the Neptune Export Lateral PLETs,” *Offshore Technology Conference*, OTC 19688, Houston, Texas, May 2008.
[8] H. Mota, “Development of In-Line PLETs for TUPI Pilot Project: Challenges and Lessons Learned,” *Offshore Technology Conference Brasil*, OTC 22182, Rio de Janeiro, Brazil, October 2011.
[9] Xie, P. et al., Overbend monitoring during deepwater S-Lay, International Journal of Offshore and Polar Engineering, 2017
[10] Xie, P. et al, Real-time strain monitoring in overbend, Proceedings of the Twenty-fifth International Ocean and Polar Engineering Conference, 2015
[11] Ivić, S. – Sensitivity analysis of S-Lay configuration, International Journal of Applied Engineering Research, 2015
[12] Xu, P. & Gong, S. (2020) – Dynamic response of S-Lay pipelines under waves, Journal of Offshore Mechanics and Arctic Engineering, 2020
[13] S. Kyriakides and E. Corona, Mechanics of Offshore Pipelines, Vol. 1: Buckling and Collapse. Oxford: Elsevier, 2007. ISBN 978-0-08-046732-0.
[14] Y. Liu and S. Kyriakides, “Effect of Geometric and Material Discontinuities on the Reeling of Pipelines,” Applied Ocean Research, vol. 65, pp. 238–250, 2017. DOI: 10.1016/j.apor.2017.04.004.

[15] R. Bruschi, F. Torselletti, E. Vitali, B. Marchionni, P. Ragni, and G. Skaug, "Controlling Fatigue Damage during Deepwater Installation of Inline Components," ASCE Journal of Pipeline Systems Engineering and Practice, vol. 8, no. 3, pp. 04017003, Aug. 2017.
[16] G. Kaliyaperumal, O. Fang, and D. Sealock, "A Challenging Trunkline ILT Design Driven by S-Lay Installation," Offshore Technology Conference, OTC 24411, Houston, Texas, May 2013.
[17] J. J. Jansen, "Partially Displacement Controlled Conditions in the Overbend During S-Lay Pipeline Installation," M.Sc. thesis, Delft University of Technology, Delft, Netherlands, May 2018.
[18] M. Liu, H. Zhou, B. Wang, Y.-Y. Wang, J. Bergman, B. Ayton, M. Stephens, T. Weeks, and J. Gianetto, "Strain-Based Design and Assessment in Critical Areas of Pipeline Systems with Realistic Anomalies," Final Report, Contract No. DTPH56-14-H-00003, U.S. Department of Transportation PHMSA, August 2017.
[19] H. D. Yun, R. R. Peek, P. R. Paslay, and F. F. Kopp, "Loading History Effects for Deep-Water S-Lay of Pipelines," Journal of Offshore Mechanics and Arctic Engineering, vol. 126, no. 2, pp. 156–163, May 2004. DOI: 10.1115/1.1710871.
[20] S. Ai, L. Sun, L. Tao, and S. C. Yim, "Modeling and Simulation of Deepwater Pipeline S-Lay With Coupled Dynamic Positioning," Journal of Offshore Mechanics and Arctic Engineering, vol. 140, no. 5, p. 051704, Oct. 2018. DOI: 10.1115/1.4040049.
[21] Orcina Ltd, "Orcaflex for Pipelay", https://www.orcina.com/wp-content/uploads/OrcaFlex-for-pipelay.pdf, accessed June 2026

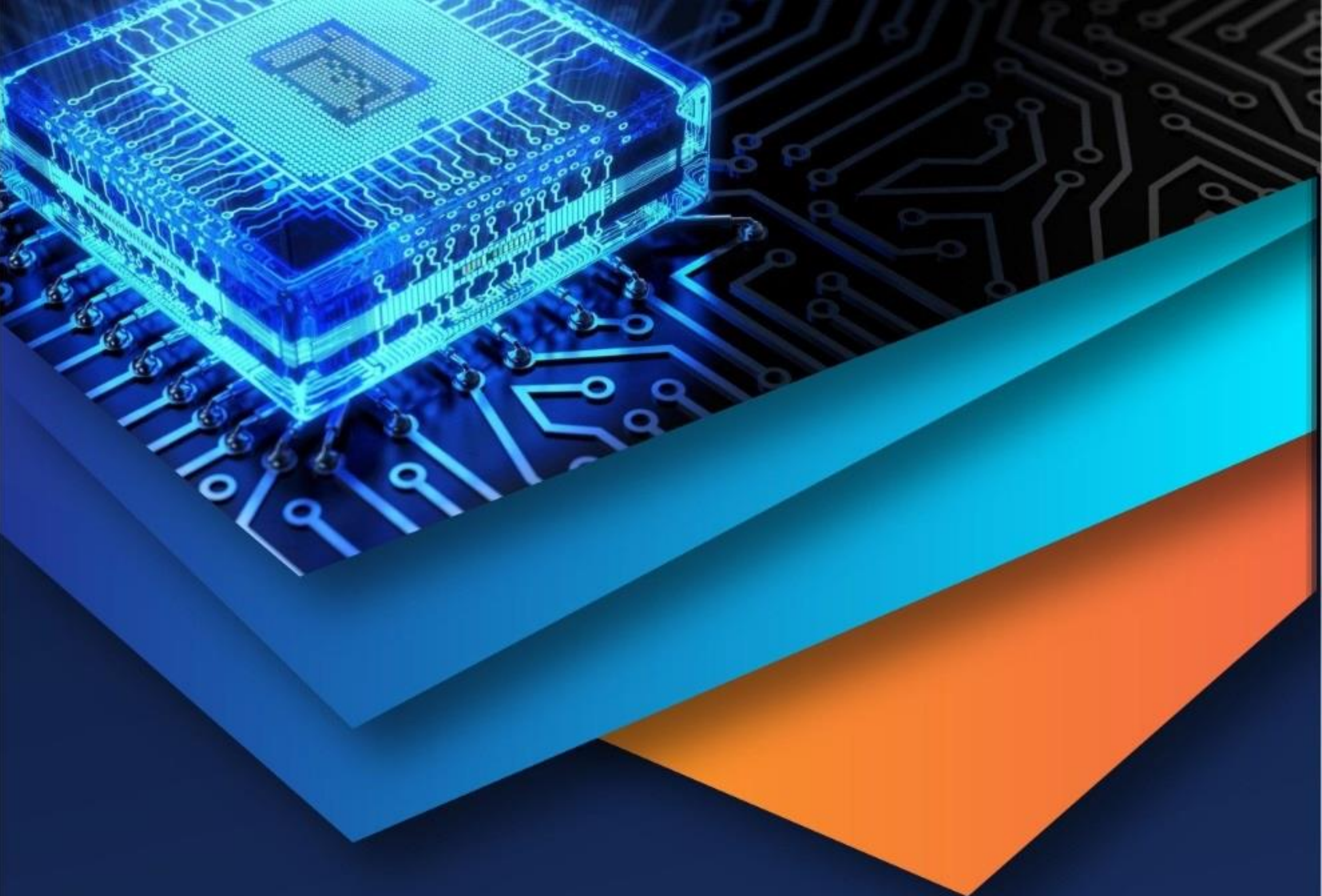

10.22214/IJRASET

45.98

IMPACT FACTOR: 7.129

IMPACT FACTOR: 7.429

INTERNATIONAL JOURNAL FOR RESEARCH

IN APPLIED SCIENCE & ENGINEERING TECHNOLOGY

Call : 08813907089 (24*7 Support on Whatsapp)